

1 **Hidden biosphere in an oxygen-deficient Atlantic open ocean eddy: Future implications of ocean**
2 **deoxygenation on primary production in the eastern tropical North Atlantic**

3

4 C. R. Löscher^{1*}, M. A. Fischer^{1†}, S. C. Neulinger^{1†}, B. Fiedler², M. Philippi¹, F. Schütte², A. Singh^{2#}, H.
5 Hauss², J. Karstensen², A. Körtzinger^{2,3}, S. Künzel⁴, R. A. Schmitz¹

6 [1] Institute for General Microbiology, Kiel, Germany

7 [2] GEOMAR, Helmholtz Centre for Ocean Research Kiel, Kiel University, Germany

8 # Now at: Physical Research Laboratory, Geosciences Division, Ahmedabad, India 380 009

9 [3] Christian-Albrechts-Universität zu Kiel, Kiel, Germany

10 [4] Max Planck Institute for Evolutionary Biology, Plön, Germany

11

12 * Correspondence should be addressed to cloescher@geomar.de

13 † Equal contribution.

14

15 The eastern tropical North Atlantic (ETNA) is characterized by a highly productive coastal upwelling
16 system and a moderate oxygen minimum zone with lowest open ocean oxygen (O₂) concentrations of
17 approximately 40 μmol kg⁻¹. The recent discovery of re-occurring mesoscale eddies with close to anoxic
18 O₂ concentrations (<1 μmol kg⁻¹) located just below the mixed layer has challenged our understanding of
19 O₂ distribution and biogeochemical processes in this area.

20 Here, we present the first microbial community study from a deoxygenated anticyclonic modewater eddy
21 in the open waters of the ETNA. In the eddy, we observed significantly lower bacterial diversity compared
22 to surrounding waters, along with a significant community shift. We detected enhanced primary
23 productivity in the surface layer of the eddy indicated by elevated chlorophyll concentrations and carbon
24 uptake rates of up to three times as high as in surrounding waters. Carbon uptake rates below the euphotic
25 zone correlated to the presence of a specific high-light ecotype of *Prochlorococcus*, which is usually
26 underrepresented in the ETNA. Our data indicate that high primary production in the eddy fuels export
27 production and supports enhanced respiration in a specific microbial community at shallow depths, below
28 the mixed layer base. The O₂-depleted core waters eddy promoted transcription of the key gene for
29 denitrification, *nirS*. This process is usually absent from the open ETNA waters.

30 In light of future projected ocean deoxygenation, our results show that even distinct events of anoxia have
31 the potential to alter microbial community structure with critical impacts on primary productivity and
32 biogeochemical processes of oceanic water bodies.

33

34 1 Introduction

35 The eastern tropical North Atlantic (ETNA) region is influenced by an eastern boundary upwelling system
36 (EBUS) off northwest Africa, which along with nutrient supply via Saharan dust deposition, fuels one of
37 the most productive ocean regions in the world. A moderate oxygen minimum zone (OMZ) is associated
38 with this EBUS, with lowest oxygen (O_2) concentrations just below $40 \mu\text{mol kg}^{-1}$ present at intermediate
39 depths (Chavez and Messié, 2009; Jickells et al., 2005; Karstensen et al., 2008).

40 O_2 records over several years from the Cape Verde Ocean Observatory (CVOO) mooring (located at 17°
41 $35'N$, $24^\circ 15'W$, Fig. 1) confirmed the well-ventilated character of the ETNA. However, the observation
42 of distinct events of very low- O_2 concentrations ($<1 \mu\text{mol kg}^{-1}$) at depths around 40 to 100 m over periods
43 of more than one month challenged our understanding of the biogeochemistry in that area (Karstensen et
44 al., 2015a). The meridional current structure observed during these low- O_2 events revealed the passage of
45 anticyclonic modewater eddies (ACME) crossing the CVOO mooring (Karstensen et al., 2015a). The
46 ocean is filled with eddies (Chelton et al., 2011) but only a few of them have the dynamical and
47 biogeochemical boundary conditions that support formation of a low- O_2 core. Anomalous low salinity
48 within the ETNA low- O_2 eddies suggested the water mass originated from the EBUS off Mauritania,
49 which was confirmed by analyzing sea-level anomaly data. In combination with other data from the
50 upwelling region, Karstensen et al. (2015a) showed that O_2 concentrations decreased over a period of a
51 few months during westward propagation of the eddies into the open north Atlantic Ocean. Respiration in
52 these eddies was estimated to be about three to five times higher than typical subtropical gyre values
53 (Karstensen et al., 2008).

54

55 Mesoscale eddies are increasingly recognized as biogeochemical hot-spots of basin-wide relevance for the
56 world's oceans (Altabet et al., 2012; Baird et al., 2011; Chelton et al., 2011; McGillicuddy et al.,
57 2007; Oschlies and Garcon, 1998; Stramma et al., 2013). Upward nutrient supply to the euphotic zone
58 through mesoscale eddy dynamics enables intense primary productivity (Lévy et al., 2012; Lévy et al.,
59 2001; McGillicuddy et al., 2007). Classically, primary producers in the ETNA open waters area are
60 dominated by a range of diatom clades, flagellates and cyanobacteria (Franz et al., 2012), but so far no
61 specific information on the primary producers in productive ETNA eddies has been reported. As a result
62 of enhanced primary production in the surface, increased organic matter export flux below the euphotic
63 zone is expected, which in turn supports increased respiration at intermediate depths. Indeed, particle
64 maxima a few meters above the O_2 minimum have been reported based on autonomous observations of

65 O₂-depleted eddies in the ETNA (Karstensen et al., 2015a) indicating enhanced organic matter export and
66 provide environments of enhanced remineralization (Ganesh et al., 2014). Observations from a low-O₂
67 eddy from the ETNA revealed a remarkable impact on all productivity-related processes in that particular
68 system (Fischer et al., 2015). Estimated productivity was three-fold higher in the surface layer compared
69 to surrounding waters along with a multiple times increase in mass flux in bathypelagic during the eddy
70 passage. Furthermore, Fiedler et al. (in prep. for this special issue) determined export flux derived from
71 carbon remineralization rates within the eddy and found a 3-4-fold enhanced export flux compared to
72 background conditions in the open-ocean ETNA.

73
74 O₂-depleted conditions are supposed to act as a critical switch for the marine microbial community, both
75 with regard to functionality and diversity. O₂ begins to limit oxidative pathways and reductive pathways
76 are induced (Stewart et al., 2011;Ulloa et al., 2012;Wright et al., 2012). A loss in microbial diversity
77 related to vertical O₂ gradients has previously been described for the Pacific Ocean (Beman and Carolan,
78 2013;Bryant et al., 2012), but to date no comparable data are available from the ETNA. O₂-loss related
79 microbial community shifts and modified functionality are supposed to favor heterotrophic communities
80 dominated by Flavobacteria, α - and γ - Proteobacteria, which efficiently recycle organic matter (Buchan et
81 al., 2014). Furthermore, marine nitrogen (N) and carbon (C) cycling are significantly altered under low O₂
82 conditions (Vaquer-Sunyer and Duarte, 2008;Wright et al., 2012). Substantial N loss (Altabet et al., 2012)
83 along with enhanced nitrous oxide production (Arévalo-Martínez et al., 2015) has been described in low-
84 O₂ eddies in the OMZ off Peru in the eastern tropical South Pacific.

85 Classically, the N cycle in the open ETNA is assumed to be dominated by nitrification. An N loss signal is
86 not present due to comparably high background O₂ concentrations ($\geq 40 \mu\text{mol kg}^{-1}$), (Löscher et al.,
87 2012;Ryabenko et al., 2012). However, any drop in O₂ concentration in the water column, as potentially
88 induced by the low-O₂ eddies, could potentially activate anammox and/or denitrification. During recent
89 decades, the ETNA OMZ has been expanding both in terms of vertical extent and intensity and is
90 predicted to expand further in the future (Stramma et al., 2008) with unknown consequences for the
91 ecology and biogeochemistry of that system. Thus, it is critical to understand the biogeochemical response
92 to changing O₂ concentrations in that region.

93
94 In this study, we investigated differences in microbial community structure in an O₂-depleted eddy,
95 surrounding ETNA open waters, and upwelled waters on the Mauritanian shelf. This was achieved using a
96 combined high-throughput 16S rDNA amplicon sequencing/qPCR approach along with carbon uptake rate
97 measurements and hydrochemical observations. This study aimed to understand the microbial community
98 response to O₂ depleted conditions with regard to primary production and remineralization in these poorly-

99 described anomalies, to improve understanding of the sensitivity of the ETNA biogeochemistry to future
100 ocean deoxygenation.

101

102 2 Material and Methods

103 2.1 Data collection

104 Remotely sensed sea level anomalies (SLA), in combination with temperature and salinity data measured
105 by Argo floats (an overview is presented by Körtzinger et al., (2015) in preparation for this issue) were
106 used for general eddy identification and tracking in this area. After identification of a low-O₂ eddy
107 candidate that was propagating towards CVOO, a pre-survey was started using autonomous gliders (see
108 Karstensen et al. (2015b), in preparation for this issue). Once the glider data had confirmed the low O₂
109 concentration in the candidate eddy, a ship-based survey was started. First, we performed a survey with
110 the Cape Verdean RV *Islandia* on Mar 6, 2014 (samples from this survey are further referred to as
111 eddy_1), followed by a second survey with the German RV *Meteor* (cruise M105; Mar 19, 2014; samples
112 from this survey are further referred to as eddy_2). Moreover, the background signal (i.e. waters outside
113 the eddy) was measured, in order to compare the eddy with the typical open ocean ETNA environment.
114 For this purpose, we used metagenomic samples from the CVOO time series monitoring site (collected on
115 03/19/2014 during cruise M105). Samples from the Mauritanian shelf collected during R/V *Meteor* Cruise
116 M107 (station 675, 18.22°N/ 16.56°W, collected on 06/24/2014) represent data from the eddy formation
117 area. Station 675 was chosen according to its location within the area that Schütte et al. (2015, in
118 preparation, this issue) identified as the region of eddy formation and further because of the observed low
119 O₂ concentrations of 33.9 μmol kg⁻¹ at 115 m depth (which corresponds to a potential density of $\sigma_{\tau} = 26.4$
120 kg m⁻³, thus similar to the core density of minimal O₂ concentrations in the eddy).

121 In addition to metagenomic sampling, carbon uptake measurements were performed during the R/V
122 *Meteor* M105 survey at two stations: no. 186 (profile 10, 19.3°N, 24.77°W) and no. 190 (profile 15,
123 18.67°N, 24.87°W, see Fig. 1C, blue crosses).

124

125 2.2 Water sampling and Hydrographic parameters

126 Discrete samples for salinity, dissolved O₂ and nutrients on all surveys were taken from a CTD rosette
127 equipped with Niskin-bottles. The CTD data were calibrated against salinity samples and CTD oxygen
128 probe data (SBE 43 Clark electrode sensor) were calibrated against O₂ concentrations, determined
129 following the Winkler method using 50 or 100 mL samples. Salinity and nutrient concentrations were
130 determined as described in Grasshoff et al. (1999). The CTD on R/V *Meteor* was equipped with double
131 sensors for conductivity, temperature, and oxygen. Calibration followed standard procedures (GO-SHIP
132 Manual; (Hood et al., 2010)).

133

134 2.3 Oxygen respiration

135 In order to estimate the net O₂ consumption as a potential driver for microbiological community shifts a
136 simple calculation was performed as follows:

137

$$138 \quad (1) \Delta O_2 = O_2(S) - O_2(E)$$

139

140 where O₂(S) denotes the lowest O₂ concentration detected on the shelf ($36.69 \pm 6.91 \mu\text{mol kg}^{-1}$ at $\sigma_T = 26.3$
141 $\pm 0.15 \text{ kg m}^{-3}$, cruise M107, average of shelf stations between 18.10°N/ 16.59°W and 18.25°N/ 16.45°W).

142 This region was chosen as it was identified (Schütte et al. (2015), in preparation, this issue) to be the area
143 where the eddy most likely originated. O₂(E) denotes the lowest O₂ concentration measured in the eddy
144 core at the same potential density ($4.8 \mu\text{mol kg}^{-1}$ at $\sigma_T = 26.35 \text{ kg m}^{-3}$ during M105).

145 The daily O₂ loss rate (ΔO_{2d}) was calculated as follows, assuming a lifetime of 180 days of the eddy
146 (Schütte et al. (2015), in preparation, this issue):

147

$$148 \quad (2) \Delta O_{2d} = \Delta O_2 / 180$$

149 2.4 Chlorophyll a measurements

150 Sea water samples (0.5 – 1 L) for chlorophyll *a* (Chl *a*) analyses were filtered (200 mbar) on GF/F filters
151 (25 mm, 0.7 μm ; Whatman, Maidstone, UK). Filters were transferred to a plastic vial and 1 mL of MilliQ
152 water was added. Filters were immediately frozen at -20°C and stored for at least 24 h. Afterwards, 9 mL
153 acetone (100 %) was added to the vials and the fluorescence was measured with a Turner Trilogy
154 fluorometer (Sunnyvale, CA, USA). Calibration took place using a Chl *a* standard dilution series
155 (*Anacystis nidulans*, Walter CMP, Kiel, Germany). Chl *a* concentrations were determined as described by
156 Parsons et al. (1984).

157

158 2.5 Molecular Methods

159 Seawater samples were taken from the Niskin-Bottles at selected CTD casts. For nucleic acid purification
160 2 L seawater was rapidly filtered (exact filtration volumes and times were recorded continuously) through
161 0.2 μm polyethersulfone membrane filters (Millipore, Billerica, MA, USA). The filters were immediately
162 frozen and stored at -80°C until further analysis. Nucleic acids were purified using the Qiagen DNA/RNA
163 AllPrep Kit (Qiagen, Hilden, Germany) with modifications as previously described (Löscher et al., 2012).

164

165 Extracts of DNA and RNA were quantified using a spectrophotometer (Thermo Fisher Scientific,
166 Waltham, MA, USA). To remove DNA from RNA extracts, a DNase I treatment (Invitrogen, Carlsbad,

167 CA) was performed; purity of RNA was checked by PCR amplification before random reverse
168 transcription with the Quanti Tect® Reverse Transcription Kit (Qiagen, Hilden, Germany). HNLC, HLII
169 and other *Prochlorococcus* ecotypes were qPCR-amplified using primers and PCR conditions as
170 previously described (Ahlgren et al., 2006). Reactions were performed in technical duplicates in a final
171 volume of 12.5 µL using 0.25 µL of each primer (10 pmol µL⁻¹), 3.25 µL nuclease-free water and 6.25 µL
172 SYBR qPCR Supermix W/ROX (Life Technologies, Carlsbad, CA, USA) on a ViiA7 qPCR machine
173 (Life Technologies, Carlsbad, CA, USA) according to established protocols (Ahlgren et al., 2006; West et
174 al., 2011). TaqMan-based qPCRs were performed for picophytoplankton
175 (*Prochlorococcus/Synechococcus*) and bacteria as previously described (Suzuki et al., 2001) in a final
176 volume of 12.5 µL with primer/probe concentrations as shown elsewhere (Table 1, (West et al., 2011)),
177 but with the addition of 0.5 µL BSA (20 mg mL⁻¹) and 6.25 µL TaqMan Mix (Life Technologies,
178 Carlsbad, CA, USA). Dilution series of plasmids containing the target gene were used as standards as
179 described (Lam et al., 2007; Löscher et al., 2012). Nitrogen cycle key functional genes *amoA*, *nirS*, *hzo* and
180 *nifH* were amplified and quantified from DNA and cDNA following established protocols (Lam et al.,
181 2007; Langlois et al., 2008; Löscher et al., 2014; Löscher et al., 2012). Detection limits of qPCR assays
182 were determined from no-template controls, which were run in duplicate for each primer (and probe) set,
183 and were undetectable after 45 cycles, thus setting the theoretical detection limit of our assay mixtures to
184 one gene copy. However, detection limits additionally depend on the amount of filtered seawater per
185 sample, elution volume after extraction, and the amount of sample loaded to the qPCR assay. Based on a
186 filtration volume of 2L seawater, a detection limit of 20 copies L⁻¹ has been determined. qPCR efficiencies
187 were calculated using the formula $E = 10^{-1/\text{slope}} - 1$, and were between 95.3% and 96.8%.

188

189 2.5.1 PCR amplification of bacterial and archaeal 16S rDNA for Illumina MiSeq amplicon 190 sequencing

191 For the analysis of the bacterial community, hypervariable regions V1 and V2 of the 16S rDNA was
192 amplified from genomic DNA using the primer set 27 forward (Frank et al., 2007) and 338 reverse (Fierer
193 et al., 2008). Beside the target-specific region the primer sequence contained a linker sequence, an 8-base
194 barcode and the Illumina specific region P5 (forward primer) or P7 (reverse primer), respectively, as
195 recently described (Kozich et al. 2013). The PCR reaction mixture consisted of 13.6 µL DEPC H₂O (Roth,
196 Karlsruhe, Germany), 0.4 µL of 10 mM dNTPs (Thermo Fisher Scientific), 4 µL 5x HF-buffer (Thermo
197 Fisher Scientific, Waltham, MA, USA), 0.8 µL primers (5 µM, Eurofins, Ebersberg, Germany), 0.2 µL
198 Phusion high fidelity polymerase (2 U µL⁻¹, Thermo Fisher Scientific, Waltham, MA, USA) and 1 µL
199 genomic DNA with a concentration between 10 and 100 ng µL⁻¹. Negative controls consisted of the

200 reaction mixture as described above without the addition of DNA. PCR reaction conditions started with an
201 initial denaturation step for 5 min at 95°C followed by 30 cycles of 15 s denaturation at 95°C, 30 s primer
202 annealing at 52°C and 30 s elongation at 72°C and a final elongation at 72°C for 5 min.

203
204 For analysis of the archaeal community, hypervariable regions V5-V7 of the 16S rDNA were amplified
205 from genomic DNA using the primer set 787 forward and 1059 reverse (Yu et al., 2005) with 8-base
206 barcode and Illumina specific adapters. Reaction mixture, PCR protocol and purification were identical to
207 the amplification of bacterial community DNA amplification, the only difference was the annealing
208 temperature (58°C). Amplification was checked for correct size and band intensity on a 2.5% agarose gel.
209 Amplicons were purified using the MinElute Gel Extraction Kit (Qiagen, Hildesheim, Germany and
210 quantified on a spectrophotometer (Nanodrop 1000, Thermo Fisher Scientific, Waltham, MA, USA).
211 Pooled purified amplicons were prepared and sequenced according to the manufacturer's protocol on a
212 MiSeq Instrument using the MiSeq reagent Kit V3 chemistry (Illumina, San Diego, CA, USA). Sequences
213 were submitted to NCBI Sequence Read Archive under accession number PRJNA288724.

214 2.5.2 Sequence analysis of 16S rDNA gene amplification

215 Sequence processing was performed using mothur software version 1.32.1 (Kozich et al., 2013; Schloss et
216 al., 2009). 4,054,723 bacterial sequence read pairs could be concatenated to contiguous sequences
217 (contigs) using the command *make.contig*. Contigs containing ambiguous bases, homopolymers longer
218 than 8 bases or contigs longer than 552 bases were deleted from the dataset. Redundant sequences were
219 clustered using the command *unique.seqs*, which led to 645,444 unique sequences. Sequences were
220 consecutively aligned with *align.seqs* against a modified version of the SILVA database release 102
221 (Pruesse et al., 2007) containing only the hypervariable regions V1 and V2. The alignment was optimized
222 by removing sequences not aligning in the correct region with *screen.seqs*, and by the removal of gap-only
223 columns using *filter.seqs*. The optimized alignment contained 636,701 sequences of lengths between 255
224 and 412 bases. Rare sequences with up to 3 positional differences compared to larger sequence clusters
225 were merged with the latter by the *pre.cluster* command. Chimeric sequences were removed with the
226 implemented software UCHIME (Edgar et al., 2011) using the command *chimera.uchime*, followed by
227 *remove.seqs*.

228
229 Taxonomic classification of the remaining sequences was done using the Wang approach based on a
230 modified version of the Greengenes database (DeSantis et al., 2006) with a bootstrap threshold of 80%.
231 Sequences of archaea, chloroplasts and mitochondria were removed with *remove.lineage*. Operational
232 taxonomic units (OTUs) were formed by average neighbor clustering using the *cluster.split* command,
233 parallelizing the cluster procedure by splitting the dataset at the taxonomic order level. A sample-by-OTU

234 table was generated with *make.shared* at the 97 % sequence similarity level. The resulting table contained
235 15,509 OTUs. OTUs were classified taxonomically using the modified Greengenes database mentioned
236 above and the command *classify.otu*.

237
238 Archaeal sequences showed lower quality in the reverse read, which lead to multiple ambiguous bases in
239 the contigs formed. For this reason only the forward read starting from base 36 was used for analysis.
240 Sequence analysis was performed as described above for bacterial 16S sequences, except that the
241 alignment (*align.seqs*) was accomplished using the SILVA archaeal reference release 102 (Pruesse et al.,
242 2007) fitted for hypervariable regions V5-V7. Classification (*classify.seqs* and *classify.otu*) was conducted
243 using the RDP database file release 10 (Cole et al., 2014; Wang et al., 2007). Results and additional
244 information on the archaeal community structure are listed in the supplemental material.

245 An overview of the sequencing output is given in table S1.

246

247 2.6 Statistics

248 Low-abundance OTUs were removed to reduce noise and computation time. Statistical downstream
249 analysis was performed in R v3.1.3 (R Core Team, 2015) with custom scripts (available from the authors
250 on request). As OTUs of very low abundance only increase computation time without contributing useful
251 information, they were removed from the data set as follows: After transformation of counts in the
252 sample-by-OTU table to relative abundances (based on the total number of reads per sample), OTUs were
253 ordered by decreasing mean percentage across samples. The set of ordered OTUs for which the
254 cumulative mean percentage amounted to 99% was retained in the filtered OTU table.

255 Distribution of OTUs across samples was modeled by a set of environmental variables (Table S2) with
256 minimal interdependence. The variance in OTU composition (i.e., the extent of change in OTU abundance
257 across samples) explained by the measured environmental variables was explored by redundancy analysis
258 (RDA) with Hellinger-transformed OTU counts (Langfeldt et al., 2014; Stratil et al., 2013; Stratil et al.,
259 2014) using the R package *vegan* (Oksanen et al., 2013). In order to minimize collinearity of explanatory
260 variables in the RDA model, a subset of the recorded environmental variables was chosen according to
261 their variance inflation factor (VIF), employing *vegan*'s functions *rda* and *vif.cca*. Starting with an RDA
262 model that contained all explanatory variables, the variable with the highest VIF was iteratively
263 determined and removed from the model until all remaining explanatory variables had a VIF <2.5.

264

265 OTU distribution was subject to "Realm" depending on O₂ concentration. Model selection started with a
266 full RDA model containing all main effects and possible interactions based on the set of explanatory
267 variables with minimal collinearity. This model was simplified by backward selection with function
268 *ordistep*. The final RDA model exhibited a significant interaction effect "Realm:O₂" (see results section).

269 For plotting and indicator analysis (see below), the continuous variable “O₂” was converted into a factor
270 with two levels “high O₂” (>90 μmol L⁻¹) and “low O₂” (≤90 μmol L⁻¹); the threshold of 90 μmol L⁻¹ was
271 chosen for two reasons: (1) to obtain sample groups of fairly equal size between stations, which include
272 low O₂ parts of the water column at all sampling stations in order to enable a comparison between the
273 ETNA OMZ (outside the eddy) and the eddy OMZ. (2) 90 μmol L⁻¹ has previously described the highest
274 concentration of O₂ at which denitrification has been detected to be active (Gao et al., 2010). The presence
275 of *nirS* transcripts (see section 3.4) indicated a potential importance for denitrifiers in the eddy, therefore
276 the theoretical upper limit of 90 μmol L⁻¹ was chosen.

277
278 We determined OTUs typical for a given combination of levels of factors "Realm" and "O₂". OTUs
279 significantly correlated with any axis in the final RDA model were determined using the function *envfit*
280 with 10⁵ permutations, followed by Benjamini-Hochberg correction (false discovery rate, FDR)
281 (Benjamini and Hochberg, 1995). In order to reduce the number of tests in this procedure, OTUs were pre-
282 filtered according to their vector lengths calculated from corresponding RDA scores (scaling 1) by profile
283 likelihood selection (Zhu and Ghodsi, 2006).

284
285 OTUs significant at an FDR of 5% were further subject to indicator analysis with function *multipatt* of the
286 R package *indicspecies* v1.7.4 (De Cáceres and Legendre, 2009) with 10⁵ permutations. Indicator OTUs –
287 in analogy to indicator species *sensu* De Cáceres and Legendre (2009) – are OTUs that prevail in a certain
288 sample group (here: a level of factor “Realm” within a chosen O₂ level) while being found only irregularly
289 and at low abundance in other sample groups. In order to remove the effects of the covariate “Depth” in
290 indicator analysis, Hellinger-transformed counts of significant OTUs were first subjected to a linear
291 regression with “Depth”; residuals of this regression were then transformed to positive values by
292 subtraction of their minimum and used as input for indicator analysis.

293 3D visualizations of the RDA model were produced in kinemage format (Richardson and Richardson,
294 1992) using the R package R2Kinemage developed by S.C.N., and displayed in KiNG v2.21 (Chen et al.,
295 2009).

296
297 Diversity within samples was related to environmental variables by advanced linear regression. For alpha
298 diversity analysis, effective OTU richness (Shannon numbers equivalent, ¹D, (Jost, 2006, 2007)) was
299 calculated from the filtered OTU table. ¹D was fitted to the set of explanatory variables with minimal
300 collinearity in a generalized least squares (GLS) model using function *gls* of the R package *nlme* v3.1-120
301 (Pinheiro et al., 2015). The variable “NO₂” was square root-transformed to decrease the potential leverage
302 effect of its two highest values (0.25 μmol L⁻¹ and 0.28 μmol L⁻¹, respectively) on ¹D. Apart from main

303 effect terms, the interaction term “Realm:O₂” was included into the GLS model for comparability with
304 beta diversity analysis (see results section). The variance structure of the GLS model was chosen to
305 account for both different variances per level of “Realm” and an overall decreasing variance by “Depth”.
306 The resulting model was validated following the recommendations of Zuur et al. (2009). While only the
307 “Realm” effect was significant, the other terms were kept in the model to maintain a valid residual
308 distribution. For visualization of the (partial) effect of only factor “Realm” on ¹D, partial response
309 residuals were extracted from the full GLS model re-fitted without the “Realm” main effect. These partial
310 response residuals were then modelled by the “Realm” main effect alone, using the same variance
311 structure as for the full GLS model.

312

313 2.7 Carbon fixation rate measurements

314 Seawater incubations were performed in triplicate at two stations, one inside the eddy (station 10, M105
315 cruise) and one in ETNA open waters (station 15, M105 cruise, both stations indicated in Fig. 1C).
316 Seawater was sampled from a CTD system and directly filled into 2.8 L polycarbonate bottles (Nalgene,
317 Thermo Fisher Scientific, Waltham, MA, USA). For carbon fixation measurements, NaH¹³CO₃
318 (Cambridge Isotope Laboratories, MA, USA) was dissolved in sterile deionized water (>18.2 MΩ cm⁻¹,
319 MilliQ, Merck-Millipore, Darmstadt, Germany; 5 g/294 mL). A volume of 1 ml (2.8 L bottles) was added
320 to the incubations with a syringe (~4.4 atom % final). After amendment, bottles were stored on deck in a
321 seawater-cooled Plexiglas incubator covered with light foils (blue-lagoon, Lee filters, Andover,
322 Hampshire, UK) that mimic light intensities at corresponding sampling depths (5/10/30/70 m). Samples
323 from below the euphotic zone were stored at 12°C in the dark. The depth of the euphotic zone was
324 estimated from photosynthetically active radiation (PAR) sensor measurements from CTD profiles as the
325 depth where PAR is <1% of the surface value. This corresponded to 60 m water depth during this survey.
326 After 24 h of incubation, 1.5–2.8 L of seawater were filtered onto pre-combusted (450°C, 5 h) 25 mm
327 diameter GF/F filters (Whatman, Maidstone, UK) under gentle vacuum (-200 mbar). Filtrations were
328 stopped after 1 h since high particle load of surface water led to a clogging of the filters. Filters were oven
329 dried (50°C) for 24 h and stored over desiccant until analysis. Environmental samples of 2.8 L untreated
330 seawater were filtered and prepared in the same way to serve as blank values. For isotope analysis, GF/F
331 filters were acidified over fuming HCl overnight in a desiccator. Filters were then oven-dried for 2 h at
332 50°C and pelletized in tin cups. Samples were analysed for particulate organic carbon and nitrogen (POC
333 and PON) and isotopic composition using a CHN analyser coupled to an isotope ratio mass spectrometer.

334

335 3 Results and Discussion

336 3.1 Hydrography of low-O₂ eddy reveals similarities to shelf waters

337 As the detailed properties of the investigated eddy are described in Schütte et al. (2015, in preparation for
338 this issue) only the main characteristics are mentioned here:

339
340 The surveyed low-O₂ eddy belongs to the group of the anticyclonic modewater eddies (ACME)
341 (Karstensen et al. 2015a). It has been reported that ACME promote intense primary production in surface
342 and mixed layer waters (Mahadevan, 2014) fueled by nutrient supply to the euphotic zone. The surveyed
343 eddy had a diameter of about 100 km and was characterized by highly elevated mixed layer chlorophyll a
344 (chl_a) concentrations, a positive SLA signature (Fig. 1) and a low O₂/ low salinity core (Fig. 2). The O₂-
345 depleted core, with concentrations of less than 5 μmol kg⁻¹, was centered rather deep for an ACME at
346 ~100 m depth. Concentrations of less than 30 μmol kg⁻¹ were observed in the eddy water column between
347 70 to 150 m depth (Fig. 2, 3A), which is significantly below average O₂ concentrations in that region. O₂
348 concentrations in the core decreased over the survey period (March 2014), (see Fiedler et al. (2015) in this
349 issue, for a detailed description of O₂ properties). During the metagenomic sampling of the background
350 signal (“no eddy”) on the shelf (Meteor M107 cruise station 675, 18.22°N/ 16.56°W, Fig. 1), O₂
351 concentrations of 33.9 μmol kg⁻¹ were observed at 115 m depth, which corresponds to the potential density
352 layer of the low O₂ core in the eddy. The open ocean background minimum O₂ concentrations of about 70
353 μmol kg⁻¹ were detected at ~250 m depth at CVOO (Fig. 1). This can be considered average O₂
354 concentrations for the open ETNA (Karstensen et al., 2008).

355
356 In the low-O₂ eddy core, we observed nitrate and phosphate concentrations around twice as high as
357 background concentrations at CVOO at the same depth (Fig. 3). However, N:P ratios below the mixed
358 layer were close to Redfield stoichiometry (16.15 ± 0.63, Fig. 3) and thus comparable to surrounding
359 waters. Nitrate concentrations in the O₂-min core (~100 m depth) were similar to concentrations on the
360 Mauritanian shelf at 100 m depth (Fig. 3) and most likely generated by very efficient local
361 remineralization of nitrate from the sinking material (Karstensen et al. 2015b, in preparation for this
362 issue).

363
364 **3.2 Loss of phylogenetic diversity in low-O₂ eddy waters**

365 A critical issue regarding climate change induced pressures on ocean ecosystems is to understand the
366 effects of ocean acidification and deoxygenation on microbial communities as major drivers of the ocean’s
367 biogeochemistry (Riebesell and Gattuso, 2015). Thus, we investigated phylogenetic diversity of the
368 microbial community with a 16S rDNA amplicon sequencing approach of bacteria and archaea inside and
369 outside the eddy.

370 Although the bacterial community was dominated by Proteobacteria in all samples, there were distinct
371 differences between the community structures inside compared to outside the eddy (Fig. 4). Increased

372 abundances of the uncultivated SUP05 clade (up to 20% of proteobacterial sequences), have been
373 recovered from eddy samples compared to surrounding waters (Fig S1, Table S3). This clade is known to
374 occur frequently in O₂ depleted environments (Swan et al., 2011). Phyla such as Bacteroidetes,
375 Actinobacteria and Firmicutes were only present in the eddy and increased in relative abundance over
376 time. Those phyla were also detected in potential source waters on the shelf (Fig. S2). Interestingly, the
377 family of Pelagibacteraceae, which belong to the ubiquitous SAR11 clade (Giovannoni et al., 1990), were
378 strongly decreased in the eddy (to ~1% of all reads), compared to CVOO samples (~65% of all reads).
379 SAR11 was previously described as being sensitive to decreasing O₂ concentrations (Forth et al., 2014),
380 which may explain the absence of this classically highly abundant group from the eddy. In addition to the
381 dissimilarity in bacterial diversity, we also detected a substantial difference in archaeal community
382 composition between eddy stations and CVOO (Fig. S3). This was most obvious in samples from the
383 eddy_2 station, where Methanomicrobia dominated the archaeal community in the O₂-depleted parts of the
384 water column but was absent in CVOO samples. The presence of methanogens in the low-O₂ eddy core
385 samples may indicate potential for methanogenesis. Although the eddy has not been shown to become
386 fully anoxic, methanogenesis tolerates O₂ concentrations at low ranges (Angel et al., 2011).

387 Redundancy analysis (RDA) confirmed that the distribution of bacterial OTUs strongly differed between
388 the two eddy stations and CVOO samples (Fig. 6A; RDA model: $F_{6,24} = 4.48$, $p < .001$). Changes in OTU
389 composition mirrored the depth gradient (RDA “Depth”: $F_{1,24} = 2.08$, $p \approx .03$; Fig. 5) and were thus
390 strongly correlated to chemical (PO₄³⁻, NO₃⁻, SiO₂) and physical (T, S) properties (Fig. S4). The RDA
391 model indicates a noticeable interaction effect of habitat (“Realm”) and O₂ concentration (RDA
392 “Realm:O₂”: $F_{2,24} = 2.03$, $p \approx .02$), meaning that the “Realm” effect on bacterial community structure
393 depends on the O₂ level and vice versa. An overview of the parameters included in the RDA model is
394 given in table S2. O₂ and nutrient availability can thus be considered the major determining variables for
395 the composition of the microbial community.

396 Our results show further a significant decrease in bacterial alpha diversity in the eddy relative to CVOO
397 (Fig. 6). The community in eddy_2 samples was also markedly less diverse compared to those of the other
398 realms (Fig. 6; generalized least squares (GLS) model: $F_{7,23} = 5.37$, $p = .001$; GLS “Realm”: $F_{2,23} = 16.26$,
399 $p < .0001$). This may be attributed to an aging effect of the eddy, and corresponds to progressive O₂ loss
400 and consecutive changes in the eddy biogeochemistry. We calculated an overall O₂ loss of 0.18 μmol kg⁻¹
401 d⁻¹ at 100 m depth by respiration, when comparing the eddy core water to the potential origin waters on
402 the shelf, assuming a lifetime of 180 days for the eddy (average O₂ concentrations on the shelf from
403 Meteor M107 were 36.69 ± 6.91 μmol kg⁻¹ compared to observed minimum O₂ concentrations of 4.8 μmol
404 kg⁻¹ in the eddy core). These results are comparable to previous estimates on low O₂-eddies in that region
405 (Karstensen et al., 2015a). Likewise, Fiedler et al. (2015) also observed a significant increase in pCO₂ and
406 dissolved inorganic carbon compared to coastal waters, indicating enhanced remineralization and

407 respiration. Although our dataset does not allow differentiation between high- $p\text{CO}_2$ and low- O_2 effects on
408 the microbial community, it supports the view of a general loss in diversity. This may be attributed to a
409 direct or indirect response to factors related to deoxygenation and increasing $p\text{CO}_2$, such as the impact on
410 nutrient stoichiometry, as previously suggested (Bryant et al., 2012).

411 Hence, climate change-related ocean deoxygenation and consequent shifts in nutrient stoichiometry may
412 mean an overall loss of microbial diversity, with potential for substantial loss in the spectrum of metabolic
413 functions in the future ocean.

414

415 3.3 Specific *Prochlorococcus* clade contributes to primary production in the eddy

416 The detected ACME was characterized by shoaling of the mixed layer depth in the center of the eddy.
417 This coincided with a pronounced surface *chl a* maximum as observed by ocean color based and remotely
418 sensed *chl a* estimates (Fig. 1a, Fig. 7), which was slightly deeper (~50-70 m water depth) outside the
419 eddy. In accordance with increased *chl a* concentrations, enhanced carbon uptake was observed via direct
420 rate measurements of $\text{H}^{13}\text{CO}_3^-$ uptake which was potentially fueled by increased nutrient availability from
421 intermediate depths. We found a 3-fold increase in depth-integrated carbon uptake rate in the *chl a*
422 maximum of the eddy ($178.3 \pm 30.8 \text{ m mol C m}^{-2} \text{ d}^{-1}$) compared to surrounding waters ($59.4 \pm 1.2 \text{ mmol C}$
423 $\text{m}^{-2} \text{ d}^{-1}$).

424 While the upper *chl a* maximum in the eddy may likely be ascribed to eukaryotic primary producers such
425 as diatoms and flagellates that are widely distributed and abundant in that region (Franz et al., 2012),
426 confirmed by increased abundances of plastids in surface samples of our amplicon dataset (Table S3). A
427 secondary *chl a* maximum dominated by cyanobacteria was detected in the eddy at about 100 m water
428 depth, coinciding with the O_2 minimum.

429 The quantitative analysis of cyanobacterial primary producers by 16S rDNA-qPCR further revealed
430 dominance of a specific clade of *Prochlorococcus* in the secondary *chl a* maximum (Fig. S5 depicts
431 phylogenetic relations of detected *Prochlorococcus* clades). This ecotype has so far not been identified in
432 the ETNA and is only known from high nutrient low chlorophyll (HNLC) regions of the eastern tropical
433 Pacific Ocean (West et al., 2011). Its described adaptation to high nutrient conditions such as present in
434 this O_2 -depleted ACME points towards a selective advantage for this clade. Gene abundance of this
435 ecotype—for convenience further referred to as HNLC-PCC (results of an ecotypespecific 16S rDNA
436 based qPCR)—showed a strong correlation with chlorophyll ($R^2= 0.95, n=22$) below the euphotic zone
437 within the eddy. This correlation was not present outside the eddy, where HNLC-PCC abundance was
438 approximately one third compared to the second eddy observation (Fig. 8). The *Prochlorococcus*
439 community in surrounding waters was, however, dominated by another high-light ecotype of
440 *Prochlorococcus* (further referred to as HL-PCC (West et al., 2011)). Contrary to HNLC-PCC, HL-PCC
441 was not detected inside the eddy. The difference between the CVOO, eddy_1 and eddy_2 observations

442 points towards a community shift of *Prochlorococcus* related clades depending on specific characteristics
443 of the eddy (O₂, nutrient availability) with the potential to alter primary productivity in that region. Under
444 increasing pCO₂ levels, *Prochlorococcus* is predicted to substantially increase in abundance (Flombaum,
445 2013). Elevated pCO₂ levels in the eddy core water may therefore—apart from favorable elevated nutrient
446 concentrations—explain the additional selective advantage of specific *Prochlorococcus* clades, in this
447 case of HNLC-PCC. This may be critical as *Prochlorococcus* is one of the most abundant photosynthetic
448 organisms in the ocean and contributes to ~40% of dissolved organic carbon supporting bacterial
449 production (Bertillon et al., 2005).

450 Besides a direct impact of O₂, nutrients and pCO₂, increased abundances of *Prochlorococcus* in the eddy
451 may be explained from an interaction effect in the microbial community present in the eddy.
452 *Prochlorococcus* is supposed to play a major role in sustaining heterotrophs with organic carbon
453 compounds such as glycine and serine, thus favoring their growth (Biller et al., 2015; Carini et al., 2013).
454 Conversely, *Prochlorococcus* benefits from the presence of heterotrophs as they diminish the
455 concentration of reactive oxygen species in their immediate surroundings, which is not feasible for
456 *Prochlorococcus* due to the lack of catalase and peroxidase genes (Berube et al., 2014; Morris et al., 2008).
457 The close proximity of increased abundances of the HNLC-PCC maximum to the O₂ minimum in the eddy
458 may thus point towards a beneficial relationship between the HNLC-PCC and the heterotroph-dominated,
459 eddy core water microbial community.

460 461 3.4 Increased primary productivity promotes a specific heterotrophic microbial community in 462 underlying waters

463 We analyzed species indicative for the eddy and CVOO for either high-O₂ conditions (>90 μmol kg⁻¹) or
464 low-O₂ conditions (≤90 μmol kg⁻¹). Indicator OTUs for high O₂ in the eddy were mostly associated with
465 different clades of Proteobacteria, whereas Pelagibacteraceae dominated at CVOO in accordance with
466 several studies describing those organisms as ubiquitous in open-ocean oxic waters (Morris et al.,
467 2002; Rappé et al., 2002); (Poretsky et al., 2009; DeLong, 2009; Brown et al., 2014). High-O₂ samples of all
468 three sampling stations were dominated - as most parts of the ocean - by indicator OTUs belonging to the
469 Proteobacteria. The *Prochlorococcus* clade HNLC-PCC targeted by qPCR could be recovered in the 16S
470 rDNA amplicon sequences, as well.

471 For low-O₂ conditions, indicator species present in the eddy were mostly affiliated to the Cytophaga-
472 Flavobacteria-Bacteroides (CFB) group (Glöckner et al., 1999) (Table S4). Members of Bacteroidetes and
473 Proteobacteria (*Gramella*, *Leeuwenhoekiella marinoflava*, unclassified Comamonadaceae species) were
474 found to be indicative for the low-O₂ realm. *Gramella*-like organisms are usually a quantitatively
475 important fraction of the heterotrophic marine bacterioplankton, often attached to marine snow but also
476 found free-living in nutrient-rich microenvironments (Buchan et al., 2014). Frequently associated with

477 extensive phytoplankton blooms (Buchan et al., 2014), their ability to degrade high molecular weight
478 compounds in both the dissolved and particulate fraction of the marine organic matter pool points towards
479 a specific role in respiration processes and the marine C cycle (as described for '*Gramella forsetii*'
480 KT0803, Bauer et al. (2006). Karstensen et al. (2015a) described a particle maximum associated to the
481 low-O₂ core of those eddies which likely harbors this specific heterotrophic community. Further, in the
482 core of the ACME presented here, the integrated abundance (upper 600 m) of large aggregates was five
483 times higher than in surrounding waters (Hauss et al., 2015).

484
485 Enhanced productivity and consecutive respiration and O₂ decrease may enable N loss processes to occur
486 in the open ETNA, which have previously not been described for the ETNA waters (Löscher et al.,
487 2015; Löscher et al., 2012; Ryabenko et al., 2012). qPCR results of key gene distribution (*amoA* for
488 nitrification as sum of bacterial and archaeal nitrifiers, *nirS* as key gene for denitrification) in that area
489 show a decrease of *amoA* in the eddy, while *nirS* shows higher abundances inside the eddy with ~3000
490 copies L⁻¹ at depth of the O₂ minimum (compared to ~100 copies L⁻¹ outside the eddy). Besides a direct
491 sensitivity of nitrifiers to anoxic conditions, the decrease in *amoA* gene abundance (determined by qPCR)
492 towards the O₂ minimum in the eddy may result from an effect of elevated *p*CO₂ (see Fiedler et al. (2015),
493 this issue) and the corresponding drop in pH on ammonia due to a shift in the ammonia/ammonium
494 equilibrium. The latter has previously been described to alter the efficiency of nitrification (Beman et al.,
495 2011). Further, *nirS* transcripts as quantified by qPCR were detected in abundances up to 3600 transcripts
496 L⁻¹ in the eddy O₂ minimum, while no transcripts were detected outside the eddy (Fig. 9).

497
498 The presence and expression of *nirS* supports the view that potential for N loss is also present in the
499 usually oxic open ETNA. This is in line with another study on nitrous oxide (N₂O) production from the
500 same eddy (Grundle et al., submitted), where the authors observed massively increased N₂O
501 concentrations in the oxygen deficient eddy core waters in connection with denitrification. Observations
502 from e.g. the eastern tropical Pacific Ocean demonstrated previously that mesoscale eddies are drifting
503 hotspots of N loss (Altabet et al., 2012). This might be explained by feedback mechanisms between
504 eutrophication, enhanced primary productivity and consecutive enhanced export production, which may
505 promote denitrification in those systems as suggested by Kalvelage et al. (2013). Our results strongly
506 suggest that N loss is possible in eddy systems of that region, thus altering one major biogeochemical
507 cycle with unknown consequences for the ETNA biogeochemistry.

508 In case of the described eddy, we neither detected key genes for anammox (*hzs*, Schmid et al. (2008)) nor
509 significant abundances of the key genes for dinitrogen fixation. The latter has been investigated by
510 screening for the functional key gene, *nifH*, which has been tested for classical diazotrophs as
511 *Trichodesmium*, UCYN-A, UCYN-B, UCYN-C, gamma proteobacterial diazotrophs and DDAs; all of

512 which were not quantifiable by qPCR. This may be explained by the high availability of inorganic N
513 sources, as well as the prevalence of N:P close to the Redfield ratio of 16:1 as mentioned above.
514 Although N₂ fixation does not appear to play a role in the low-oxic core waters or adjacent surface waters
515 of the eddy, it may occur as a result of increasing N loss and resulting excess P as previously discussed for
516 other O₂ depleted marine habitats (Deutsch et al., 2007; Fernandez et al., 2011; Löscher et al., 2014; Ulloa et
517 al., 2012).

518 519 4 Conclusions

520 We investigated the microbial community structure and gene expression in a severely O₂-depleted
521 anticyclonic modewater eddy in the open waters of the ETNA OMZ region. This was then compared the
522 eddy observations to background signals from the ETNA open ocean CVOO time series site and the
523 Mauritanian upwelling region, where the eddy was likely formed.

524 A significant difference between microbial communities outside and inside the eddy along with an overall
525 loss in bacterial diversity in the low-O₂ core of the eddy was observed. Similarity was found between the
526 microbial community in the eddy core and on the shelf. This unique microbial community may shape the
527 specific character of this O₂-depleted eddy progressively over time.

528 We observed enhanced primary production in the eddy, presumably due to an increased nutrient supply
529 related to the eddy dynamics (Karstensen et al. 2015b). We found a specific HNLC ecotype of
530 *Prochlorococcus*, which may play a role in mediating inorganic C to certain organic C sources for the
531 associated heterotrophic community present in the eddy. Importantly, we found the first indication for N
532 loss processes in the ETNA region. Low-O₂ eddies in that region thus represent an isolated ecosystem in
533 the open ocean, forced by strongly elevated biological productivity, which travels with the eddy. This
534 leads to consequent enhanced respiration and further deoxygenation in its core waters.

535 At one stage the low-O₂ eddies will lose coherence and the extreme signatures will be released into and
536 mixed with the surrounding waters (Karstensen et al. 2015a). The ACME formation frequency for the
537 ETNA (12°-22°N and 15°-26°W) has been estimated to be about 2 to 3 yr⁻¹ (Schütte et al. 2015, in
538 preparation for this issue), hence no large scale impact of the eddies are expected. However, an
539 unexpected shift in elemental ratios or other anomalies, normally expected for regions with much lower
540 minimal oxygen levels than the ETNA, may be detected and explained by the dispersal of low-O₂ eddies.
541 Another factor to consider is the impact of deoxygenation of the ETNA (Stramma et al., 2008) as it may
542 result in even lower O₂ conditions to be created in the low-O₂ eddies. With regard to the distinct character
543 of the low-O₂ eddies and the critical shift in microbial diversity and biogeochemistry that occur over
544 relatively short times, this study contributes to understand and evaluate the far-reaching effects of future
545 and past ocean deoxygenation.

546

547 Author contribution

548 C.R.L. designed the study together with B.F., A.K., H.H. and J.K.; M.P. and C.R.L. validated the NGS
549 primer sets for marine samples, performed the molecular analysis, processed the molecular data and
550 analyzed hydrographic data. S.K. performed the high-throughput sequencing runs. M.A.F. and S.C.N.
551 performed bioinformatic analysis of high-throughput datasets. A.S. performed C-uptake measurements
552 and data analysis, F.S., J.K. and A.K. designed the eddy detection and tracking system. B.F., F.S., A.K.,
553 H.H. and C.R.L. planned the sampling campaign and B.F. performed hydrographical measurements and
554 analyzed the data. S.C.N. performed statistical analysis and modeling. C.R.L. wrote the manuscript with
555 input from all co-authors.

556

557

558 Acknowledgements

559 We thank the authorities of Cape Verde and Mauritania for the permission to work in their territorial
560 waters. We acknowledge the support of the captains and crews of R/V Islandia and R/V Meteor as well as
561 the chief scientist of M105, M. Visbeck, for his spontaneous support. Moreover, we acknowledge I.
562 Monteiro and M. Lohmann for performing oxygen and nutrient measurements, D. Grundle for sampling
563 on RV Islandia, C. Hoffman for technical assistance and the captains, crews and chief scientists of Meteor
564 M107, S. Sommer and M. Dengler, for providing hydrographical data. We acknowledge H. Bange, G.
565 Krahnmann and R. Kiko for helpful discussion of the results. G. Petrick, flying to Cape Verde to repair the
566 liquid N₂ generator was priceless- we thank you a lot for this personal effort! We thank T. Treude for
567 editing this manuscript. Further, we thank J. M. Beman and two anonymous reviewers for helpful
568 discussion of the manuscript and A. Paul for language editing.

569 Financial support for this study was provided by a grant from the cluster of excellence ‘The Future Ocean’
570 to C.R.L., A.K. and H.H.. Authors C.R.L., S.C.N., H.H. and M.P. were funded by the DFG Collaborative
571 Research Centre754 (www.sfb754.de). M.A.F. was funded and S.C.N. was co-funded by the BMBF
572 project BioPara funded to R.A.S (grant no. 03SF0421B), A.S. was funded by the cluster of excellence
573 ‘The Future Ocean’, B.F. was funded by the BMBF project SOPRAN (grant no. 03F0662A).

574

575 **References**

- 576 Ahlgren, N., Rocap, G., and Chisholm, S.: Measurement of Prochlorococcus ecotypes using
577 real-time polymerase chain reaction reveals different abundances of genotypes with similar light
578 physiologies, *Environmental Microbiology*, 8, 441–454, 2006.
- 579 Altabet, M. A., Ryabenko, E., Stramma, L., Wallace, D. W. R., Frank, M., Grasse, P., and Lavik,
580 G.: An eddy-stimulated hotspot for fixed nitrogen-loss from the Peru oxygen minimum zone,
581 *Biogeosciences*, 9, 4897–4908, 2012.
- 582 Angel, R., Matthies, D., and Conrad, R.: Activation of Methanogenesis in Arid Biological Soil
583 Crusts Despite the Presence of Oxygen, *PlosOne*, 6, doi:10.1371/journal.pone.0020453, 2011.
- 584 Arévalo-Martínez, D. L., Kock, A., Löscher, C. R., Schmitz R. A., and Bange, H. W.: Influence of
585 mesoscale eddies on the distribution of nitrous oxide in the eastern tropical South Pacific,
586 *Biogeosciences Discuss.*, 12, 9243-9273, doi:10.5194/bgd-12-9243-2015, 2015.
- 587 Baird, M. E., Suthers, I. M., Griffin, D. A., Hollings, B., Pattiaratchi, C., Everett, J. D., Roughan,
588 M., Oubelkheir, K., and Doblin, M.: The effect of surface flooding on the
589 physical–biogeochemical dynamics of a warm-core eddy off southeast Australia, *Deep Sea*
590 *Research Part II: Topical Studies in Oceanography*, 58, 592-605, 2011.
- 591 Bauer, M., Kube, M., Teeling, H., Richter, M., Lombardot, T., Allers, E., Würdemann, C. A.,
592 Quast, C., Kuhl, H., Knaust, F., Woebken, D., Bischof, K., Mussmann, M., Choudhuri, J. V.,
593 Meyer, F., Reinhardt, R., Amann, R. I., and Glöckner, F. O.: Whole genome analysis of the
594 marine Bacteroidetes 'Gramella forsetii' reveals adaptations to degradation of polymeric organic
595 matter, *Environ Microbiol.*, 8, 2201-2213, 2006.
- 596 Beman, J. M., Chow, C. E., King, A. L., Feng, Y. Y., Fuhrman, J. A., Andersson, A., Bates, N. R.,
597 Popp, B. N., and Hutchins, D. A.: Global declines in oceanic nitrification rates as a consequence
598 of ocean acidification, *Proc. Natl. Acad. Sci. U. S. A.*, 108, 208-213, 10.1073/pnas.1011053108,
599 2011.
- 600 Beman, J. M., and Carolan, M. T.: Deoxygenation alters bacterial diversity and community
601 composition in the ocean's largest oxygen minimum zone, *Nature Communications*, 4,
602 doi:10.1038/ncomms3705, 2013.
- 603 Benjamini, Y., and Hochberg, Y.: Controlling the false discovery rate: A practical and powerful
604 approach to multiple testing, *Journal of the Royal Statistical Society: Series B (Statistical*
605 *Methodology)*, 57, 289-300, 1995.
- 606 Bertillon, S., Berglund, O., Pullin, M. J., and Chisholm, S. W.: Release of dissolved organic
607 matter by Prochlorococcus, *ie et milieu - Life and environment* 55, 225-231, 2005.
- 608 Berube, P. M., Biller, S. J., Kent, A. G., Berta-Thompson, J. W., Roggensack, S. E., Roache-
609 Johnson, K. H., Ackerman, M., Moore, L. R., Meisel, J. D., Sher, D., Thompson, L. R., Campbell,
610 L., Martiny A., and Chisholm, S. W.: Physiology and evolution of nitrate acquisition in
611 Prochlorococcus, *ISME J*, <http://dx.doi.org/10.1038/ismej.2014.211>, 2014.

- 612 Biller, S. J., Berube, P. M., Lindell, D., and Chisholm, S. W.: Prochlorococcus: the structure and
613 function of collective diversity, *Nat Rev Micro*, 13, 13-27, 2015.
- 614 Brown, M. V., Ostrowski, M., Grzymski, J. J., and Lauro, F. M.: A trait based perspective on the
615 biogeography of common and abundant marine bacterioplankton clades, *Marine Genomics*, 15,
616 17-28, 2014.
- 617 Bryant, J. A., Stewart, F. J., Eppley, J. M., and DeLong, E. F.: Microbial community phylogenetic
618 and trait diversity declines with depth in a marine oxygen minimum zone, *Ecology*, 93, 1659-
619 1673, 2012.
- 620 Buchan, A., LeClerc, G. R., Gulvik, C. A., and González, J. M.: Master recyclers: features and
621 functions of bacteria associated with phytoplankton blooms, *Nat Rev Microbiol.* , 12, 686-698,
622 doi: 10.1038/nrmicro3326, 2014.
- 623 Carini, P., Steindler, L., Beszteri, S., and Giovannoni, S. J.: Nutrient requirements for growth of
624 the extreme oligotroph 'Candidatus Pelagibacter ubique' HTCC1062 on a defined medium, *ISME*
625 *J*, 7, 592–602, 2013.
- 626 Chavez, F. P., and Messié, M.: A comparison of Eastern Boundary Upwelling Ecosystems,
627 *Progress in Oceanography*, 83, 80-96, 2009.
- 628 Chelton, D. B., Gaube, P., Schlax, M. G., Early, J. J., and Samelson, R. M.: The Influence of
629 Nonlinear Mesoscale Eddies on Near-Surface Oceanic Chlorophyll, *Science*, 334, 328–332,
630 2011.
- 631 Chen, V. B., Davis, I. W., and Richardson, D. C.: KING (Kinemage, Next Generation): A versatile
632 interactive molecular and scientific visualization program, *Prot Sci*, 18, 2403-2409,
633 10.1002/pro.250, 2009.
- 634 Cole, J. R., Wang, Q., Fish, J. A., Chai, B., McGarrell, D. M., Sun, Y., Brown, C. T., Porras-
635 Alfaro, A., Kuske, C. R., and Tiedje, J. M.: Ribosomal Database Project: data and tools for high
636 throughput rRNA analysis, *Nucleic Acids Res.*, 42, 633-642, doi: 10.1093/nar/gkt1244, 2014.
- 637 De Cáceres, M., and Legendre, P.: Associations between species and groups of sites: indices
638 and statistical inference, *Ecology*, 90, 3566-3574, 10.1890/08-1823.1, 2009.
- 639 DeLong, E. F.: The microbial ocean from genomes to biomes, *Nature*, 459, 200-206,
640 10.1038/nature08059, 2009.
- 641 DeSantis, T. Z., Hugenholtz, P., Larsen, N., Rojas, M., Brodie, E. L., Keller, K., Huber, T., Dalevi,
642 D., Hu, P., and Andersen, G. L.: Greengenes, a chimera-checked 16S rRNA gene database and
643 workbench compatible with ARB, *Applied and environmental microbiology*, 72, 5069–5072,
644 10.1128/aem.03006-05, 2006.
- 645 Deutsch, C., Sarmiento, J. L., Sigman, D. M., Gruber, N., and Dunne, J. P.: Spatial coupling of
646 nitrogen inputs and losses in the ocean, *Nature*, 445, 163-167, 10.1038/nature05392, 2007.

- 647 Edgar, R. C., Haas, B. J., Clemente, J. C., Quince, C., and Knight, R.: UCHIME improves
648 sensitivity and speed of chimera detection, *Bioinformatics* 27, d2194–2200,
649 10.1093/bioinformatics/btr381, 2011.
- 650 Fernandez, C., Farias, L., and Ulloa, O.: Nitrogen Fixation in Denitrified Marine Waters, *Plos*
651 *One*, 6, 9, e20539,10.1371/journal.pone.0020539, 2011.
- 652 Fiedler, B., Grundle, D., Hauss, H., Krahnemann, G., Schütte, F., Monteiro, I., Silva, P., Vieira, N.,
653 and Körtzinger, A.: Biogeochemistry of oxygen depleted mesoscale Eddies in the open eastern
654 tropical North Atlantic In prep for *Biogeosciences Discussion*, 2015.
- 655 Fierer, N., Hamady, M., Lauber, C. L., and Knight, R.: The influence of sex, handedness, and
656 washing on the diversity of hand surface bacteria, *Proc. Natl. Acad. Sci. U. S. A.*, 105, 17994–
657 17999, 10.1073/pnas.0807920105, 2008.
- 658 Fischer, G., Karstensen, J., Romero, O., Baumann, K.-H., Donner, B., Hefter, J., Mollenhauer,
659 G., Iversen, M., Fiedler, B., Monteiro, I., and Körtzinger, A.: Bathypelagic particle flux signatures
660 from a suboxic eddy in the oligotrophic tropical North Atlantic: production, sedimentation and
661 preservation, *Biogeosciences Discuss.*, 12, 18253-18313, 10.5194/bgd-12-18253-2015, 2015.
- 662 Flombaum, P., et al. : Present and future global distributions of the marine Cyanobacteria
663 *Prochlorococcus* and *Synechococcus*, *Proc. Natl. Acad. Sci. USA.*, 110, 9824–9829, 2013.
- 664 Forth, M., Liljebladh, B., Stigebrandt, A., Hall, P. O. J., and Treusch, A. H.: Effects of ecological
665 engineered oxygenation on the bacterial community structure in an anoxic fjord in western
666 Sweden, *ISME Journal*, 9, DOI: 10.1038/ismej.2014.172 2014.
- 667 Frank, D. N., St Amand, A. L., Feldman, R. A., Boedeker, E. C., Harpaz, N., and Pace, N. R.:
668 Molecular-phylogenetic characterization of microbial community imbalances in human
669 inflammatory bowel diseases, *Proc. Natl. Acad. Sci. U. S. A.*, 104, 13780–13785,
670 10.1073/pnas.0706625104, 2007.
- 671 Franz, J. M. S., Hauss, H., Sommer, U., Dittmar, T., and Riebesell, U.: Production, partitioning
672 and stoichiometry of organic matter under variable nutrient supply during mesocosm
673 experiments in the tropical Pacific and Atlantic Ocean, *Biogeosciences*, 9, 4629-4643, 2012.
- 674 Ganesh, S., Parris, D. J., DeLong, E. F., and Stewart, F. J.: Metagenomic analysis of size-
675 fractionated picoplankton in a marine oxygen minimum zone, *ISME J*, 8, 187-211, 2014.
- 676 Gao, H., Schreiber, F., Collins, G., Jensen, M. M., Kostka, J. E., Lavik, G., de Beer, D., Zhou, H.-
677 Y., and Kuypers, M. M. M.: Aerobic denitrification in permeable Wadden Sea sediments, *ISME J*,
678 4, 417-426, 2010.
- 679 Giovannoni, S. J., Britschgi, T. B., Moyer, C. L., and Field, K. G.: Genetic diversity in Sargasso
680 Sea bacterioplankton, *Nature*, 345, 60–63, doi:10.1038/345060a0, 1990.

681 Glöckner, F. O., Fuchs, B. M., and Amann, R.: Bacterioplankton compositions of lakes and
682 oceans: a first comparison based on fluorescence in situ hybridization, *Environ Microbiol.*, 65,
683 3721–3726, 1999.

684 Grasshoff, G., Kremling, K., Erhardt, M. : *Methods of seawater analysis*, 3 ed., Wiley VCH,
685 Weinheim, 1999.

686 Grundle, D. S., Löscher, C. R., Krahnemann, G., Altabet, M. A., Bange, H. W., Karstensen, J.,
687 Körtzinger, A., and Fiedler, B.: Extreme N₂O activity in an oxygenated ocean, submitted.

688 Hauss, H., Christiansen, S., Schütte, F., Kiko, R., Edvam Lima, M., Rodrigues, E., Karstensen,
689 J., Löscher, C. R., Körtzinger, A., and Fiedler, B.: Dead zone or oasis in the open ocean?
690 Zooplankton distribution and migration in low-oxygen medowater eddies, *Biogeosciences*
691 *Discuss.*, 12, 18315-18344, doi:10.5194/bgd-12-18315-2015, 2015.

692 Hood, E. M., Sabine, C. L., and Sloyan, B. M.: *The GO-SHIP Repeat Hydrography Manual: A*
693 *Collection of Expert Reports and Guidelines*, 2010.

694 Jickells, T. D., An, Z. S., Andersen, K. K., Baker, A. R., Bergametti, G., Brooks, N., Cao, J. J.,
695 Boyd, P. W., Duce, R. A., Hunter, K. A., Kawahata, H., Kubilay, N., laRoche, J., Liss, P. S.,
696 Mahowald, N., Prospero, J. M., Ridgwell, A. J., Tegen, I., and Torres, R.: Global iron
697 connections between desert dust, ocean biogeochemistry, and climate, *Science*, 308, 67-71,
698 2005.

699 Jost, L.: Entropy and diversity, *Oikos*, 113, 363-375, DOI 10.1111/j.2006.0030-1299.14714.x,
700 2006.

701 Jost, L.: Partitioning diversity into independent alpha and beta components, *Ecology*, 88, 2427-
702 2439, 10.1890/06-1736.1, 2007.

703 Kalvelage, T., Lavik, G., Lam, P., Contreras, S., Artega, L., Löscher, C. R., Oeschlies, A.,
704 Paulmier, A., Stramma, L., and Kuypers, M. M. M.: Nitrogen cycling driven by organic matter
705 export in the South Pacific oxygen minimum zone, *Nature Geosci*, 6, 228-234, 2013.

706 Karstensen, J., Stramma, L., and Visbeck, M.: Oxygen minimum zones in the eastern tropical
707 Atlantic and Pacific oceans, *Progress in Oceanography*, 77, 331-350,
708 10.1016/j.pocean.2007.05.009, 2008.

709 Karstensen, J., Fiedler, B., Schütte, F., Brandt, P., Körtzinger, A., Fischer, G., Zantopp, R.,
710 Hahn, J., Visbeck, M., and Wallace, D.: Open ocean dead-zone in the tropical North Atlantic
711 Ocean, *Biogeosciences Discussion*, 12, 2597-2605, doi:10.5194/bg-12-2597-2015, 2015a.

712 Karstensen, J., Schütte, F., Pietri, A., Krahnemann, G., Fiedler, B., Körtzinger, A., Löscher, C. R.,
713 Grundle, D., and Hauss, H.: Anatomy of open ocean dead-zones based on high-resolution
714 multidisciplinary glider data, In prep for *Biogeosciences Discussion*, 2015b.

715 Kozich, J. J., Westcott, S. L., Baxter, N. T., Highlander, S. K., and Schloss, P. D.: Development
716 of a dual-index sequencing strategy and curation pipeline for analyzing amplicon sequence data
717 on the MiSeq Illumina sequencing platform, *Appl. Environ. Microbiol.*, 79, 5112–5120,
718 10.1128/aem.01043-13, 2013.

719 Lam, P., Jensen, M. M., Lavik, G., McGinnis, D. F., Muller, B., Schubert, C. J., Amann, R.,
720 Thamdrup, B., and Kuypers, M. M. M.: Linking crenarchaeal and bacterial nitrification to
721 anammox in the Black Sea, *Proc. Natl. Acad. Sci. U. S. A.*, 104, 7104-7109,
722 10.1073/pnas.0611081104, 2007.

723 Langfeldt, D., Neulinger, S. C., Heuer, W., Staufienbiel, I., Künzel, S., Baines, J. F., Eberhard, J.,
724 and Schmitz, R. A.: Composition of microbial oral biofilms during maturation in young healthy
725 adults, *PlosOne*, 9, e87449, 10.1371/journal.pone.0087449, 2014.

726 Langlois, R. J., Hummer, D., and LaRoche, J.: Abundances and distributions of the dominant
727 *nifH* phylotypes in the Northern Atlantic Ocean, *Applied and Environmental Microbiology*, 74,
728 1922-1931, 10.1128/aem.01720-07, 2008.

729 Lévy, M., Klein, P., and Treguier, A.-M.: Impacts of sub-mesoscale physics on phytoplankton
730 production and subduction, *J. Mar. Res.*, 59, 535-565, doi: 10.1357/002224001762842181,
731 2001.

732 Lévy, M., Ferrari, R., Franks, P. J. S., Martin, A. P., and Riviere, P.: Bringing physics to life at the
733 submesoscale, *Geophysical Research Letters*, 39, 10.1029/2012gl052756, 2012.

734 Löscher, C. R., Kock, A., Könneke, M., LaRoche, J., Bange, H. W., and Schmitz, R. A.:
735 Production of oceanic nitrous oxide by ammonia-oxidizing archaea, *Biogeosciences* 9, 2419-
736 2429, 2012.

737 Löscher, C. R., Großkopf, T., Desai, F., Gill, D., Schunck, H., Croot, P., Schlosser, C., Neulinger,
738 S. C., Lavik, G., Kuypers, M. M. M., LaRoche, J., and Schmitz, R. A.: Facets of diazotrophy in
739 the oxygen minimum zone off Peru, *ISME J*, 8, 2180-2192, doi: 10.1038/ismej.2014.71, 2014.

740 Löscher, C. R., Bange, H. W., Schmitz R. A., Callbeck, C. M., Engel, A., Hauss, H., Kanzow, T.,
741 Kiko, R., Lavik, G., Loginova, A., Melzner, F., Neulinger, S. C., Pahlow, M., Riebesell, U.,
742 Schunck, H., Thomsen, S., and Wagner, H.: Water column biogeochemistry of oxygen minimum
743 zones in the eastern tropical North Atlantic and eastern tropical South Pacific Oceans
744 *Biogeosciences Discussion*, 12, 4495-4556, doi:10.5194/bgd-12-4495-2015, 2015.

745 Mahadevan: Ocean science: Eddy effects on biogeochemistry, *Nature Geoscience*, 506, 168-
746 169, doi:10.1038/nature13048, 2014.

747 McGillicuddy, D. J., Anderson, L. A., Bates, N. R., Bibby, T., Buesseler, K. O., Carlson, C. A.,
748 Davis, C. S., Ewart, C., Falkowski, P. G., Goldthwait, S. A., Hansell, D. A., Jenkins, W. J.,
749 Johnson, R., Kosnyrev, V. K., Ledwell, J. R., Li, Q. P., Siegel, D. A., and Steinberg, D. K.:
750 Eddy/wind interactions stimulate extraordinary mid-ocean plankton blooms, *Science*, 316, 1021-
751 1026, 10.1126/science.1136256, 2007.

752 Morris, J. J., Kirkegaard, R., Szul, M. J., Johnson, Z. I., and Zinser, E. R.: Facilitation of robust
753 growth of *Prochlorococcus* colonies and dilute liquid cultures by 'helper' heterotrophic bacteria,
754 *Appl. Environ. Microbiol.*, 74, 4530–4534, 2008.

755 Morris, R. M., Rappé, M. S., Connon, S. A., Vergin, K. L., Siebold, W. A., Carlson, C. A., and
756 Giovannoni, S. J.: SAR11 clade dominates ocean surface bacterioplankton communities, *Nature*
757 420, 806-810, doi:10.1038/nature01240, 2002.

758 Oksanen, J., Blanchet, F. G., Kindt, R., Legendre, P., and Minchin, P. R.: *vegan: Community*
759 *ecology package. R package version 2.0-6.*, 2013.

760 Oschlies, A., and Garçon, V.: Eddy-induced enhancement of primary production in a model of
761 the North Atlantic Ocean, *Nature*, 394, 266–269, 1998.

762 Pinheiro, J. C., Bates, D. M., DebRoy, S., Sarkar, D., and R Core Team: *nlme: Linear and*
763 *nonlinear mixed effects models, R package version 3.1-120 ed.*, 2015.

764 Poretsky, R. S., Hewson, I., Sun, S. L., Allen, A. E., Zehr, J. P., and Moran, M. A.: Comparative
765 day/night metatranscriptomic analysis of microbial communities in the North Pacific subtropical
766 gyre, *Environmental Microbiology*, 11, 1358-1375, 10.1111/j.1462-2920.2008.01863.x, 2009.

767 Pruesse, E., Quast, C., Knittel, K., Fuchs, B. M., Ludwig, W., Peplies, J., and Glöckner, F. O.:
768 SILVA: a comprehensive online resource for quality checked and aligned ribosomal RNA
769 sequence data compatible with ARB, *Nucleic acids research*, 35, 7188–7196,
770 10.1093/nar/gkm864, 2007.

771 R Core Team: *R: A language and environment for statistical computing*, R Foundation for
772 *Statistical Computing*, Vienna, Austria, 2015.

773 Rappé, M. S., Connon, S. A., Vergin, K. L., and Giovannoni, S. J.: Cultivation of the ubiquitous
774 SAR11 marine bacterioplankton clade, *Nature*, 418, 630-633 doi:10.1038/nature00917, 2002.

775 Richardson, D. C., and Richardson, J. S.: The kinemage: A tool for scientific communication,
776 *Protein Science*, 1, 3-9, 10.1002/pro.5560010102, 1992.

777 Riebesell, U., and Gattuso, J.-P.: Lessons learned from ocean acidification research, *Nature*
778 *Climate Change*, 5, 2015.

779 Ryabenko, E., Kock, A., Bange, H. W., Altabet, M. A., and Wallace, D. W. R.: Contrasting
780 biogeochemistry of nitrogen in the Atlantic and Pacific oxygen minimum zones, *Biogeosciences*
781 9, 203-215, 2012.

782 Schloss, P. D., Westcott, S. L., Ryabin, T., Hall, J. R., Hartmann, M., and al., e.: Introducing
783 *mothur: Open-source, platform-independent, community-supported software for describing and*
784 *comparing microbial communities*, *Applied and Environmental Microbiology*, 75, 7537–7541, doi:
785 10.1128/aem.01541-09 2009.

786 Schmid, M. C., Hooper, A. B., Klotz, M. G., Woebken, D., Lam, P., Kuypers, M. M. M.,
787 Pommerening-Roeser, A., op den Camp, H. J. M., and Jetten, M. S. M.: Environmental detection
788 of octahaem cytochrome c hydroxylamine/hydrazine oxidoreductase genes of aerobic and
789 anaerobic ammonium-oxidizing bacteria, *Environmental Microbiology*, 10, 3140-3149,
790 10.1111/j.1462-2920.2008.01732.x, 2008.

791 Schütte, F., Karstensen, J., Krahnemann, G., Fiedler, B., Brandt, P., Visbeck, M., and Körtzinger,
792 A.: Characterization of “dead-zone eddies” in the tropical North Atlantic Ocean, in prep for
793 *Biogeosciences Discussion*, 2015.

794 Stewart, F. J., Ulloa, O., and DeLong, E. F.: Microbial metatranscriptomics in a permanent
795 marine oxygen minimum zone, *Environ Microbiol*, 14, 23-40, 10.1111/j.1462-2920.2010.02400.x,
796 2011.

797 Stramma, L., Johnson, G. C., Sprintall, J., and Mohrholz, V.: Expanding oxygen-minimum zones
798 in the tropical oceans, *Science*, 320, 655-658, 10.1126/science.1153847, 2008.

799 Stramma, L., Bange, H. W., Czeschel, R., Lorenzo, A., and Frank, M.: On the role of mesoscale
800 eddies for the biological productivity and biogeochemistry in the eastern tropical Pacific Ocean
801 off Peru, *Biogeosciences*, 10, 7293-7306, doi:10.5194/bg-10-7293-2013, 2013.

802 Stratil, S. B., Neulinger, S. C., Knecht, H., Friedrichs, A. K., and Wahl, M.: Temperature-driven
803 shifts in the epibiotic bacterial community composition of the brown macroalga *Fucus*
804 *vesiculosus*. , *MicrobiologyOpen*, 10.1002/mbo1003.1079, 2013.

805 Stratil, S. B., Neulinger, S. C., Knecht, H., Friedrichs, A. K., and Wahl, M.: Salinity affects
806 compositional traits of epibacterial communities on the brown macroalga *Fucus vesiculosus*,
807 *FEMS Microbiology Ecology*, 88, 272–279, 10.1111/1574-6941.12292, 2014.

808 Suzuki, M., Preston, C., Chavez, F., and DeLong, E.: Quantitative mapping of bacterioplankton
809 populations in seawater: field tests across an upwelling plume in Monterey Bay, *Aquatic*
810 *Microbial Ecology*, 24, 117–127, 2001.

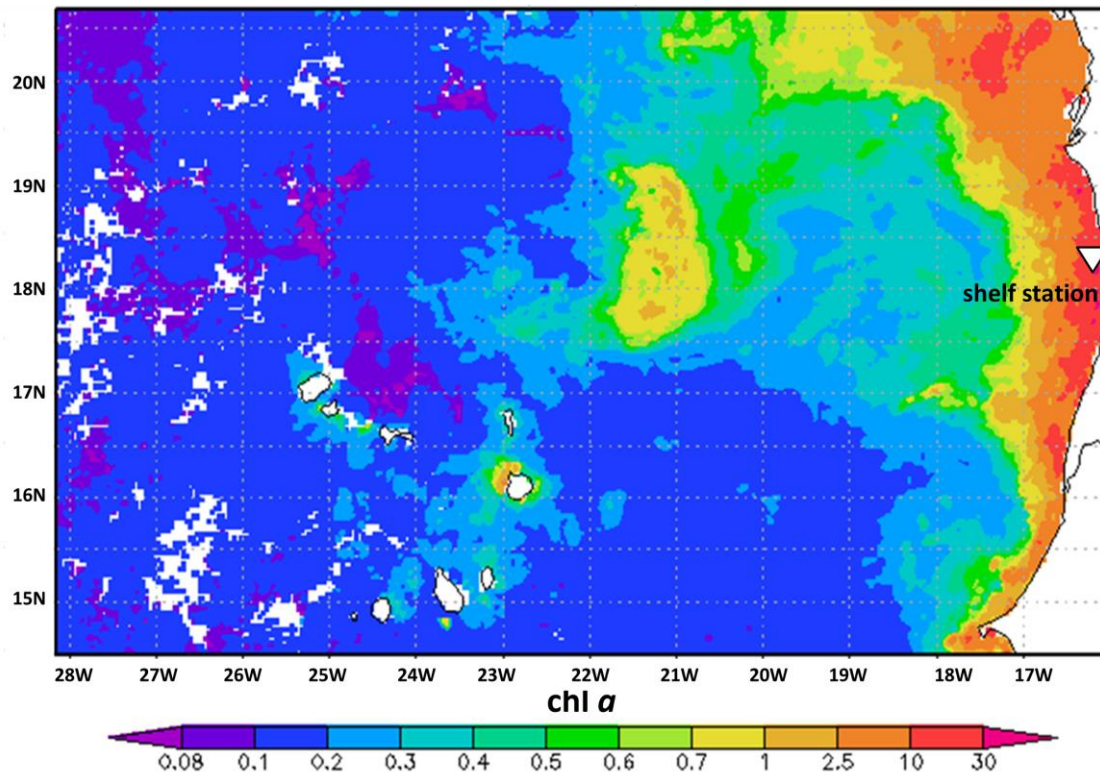
811 Swan, B. K., Martinez-Garcia, M., Preston, C. M., Sczyrba, A., Woyke, T., Lamy, D., Reinthaler,
812 T., Poulton, N. J., Masland, E. D. P., Gomez, M. L., Sieracki, M. E., DeLong, E. F., Herndl, G. J.,
813 and Stepanauskas, R.: Potential for chemolithoautotrophy among ubiquitous bacteria lineages in
814 the dark ocean, *Science*, 333, 1296–1300, 10.1126/science.1203690, 2011.

815 Ulloa, O., Canfield, D. E., DeLong, E. F., Letelier, R. M., and Stewart, F. J.: Microbial
816 oceanography of anoxic oxygen minimum zones, *Proc. Natl. Acad. Sci. U. S. A.*, 109, 15996-
817 16003, 10.1073/pnas.1205009109, 2012.

818 Vaquer-Sunyer, R., and Duarte, C. M.: Thresholds of hypoxia for marine biodiversity, *Proc. Natl.*
819 *Acad. Sci. USA.* , 105, 15452–15457, 2008.

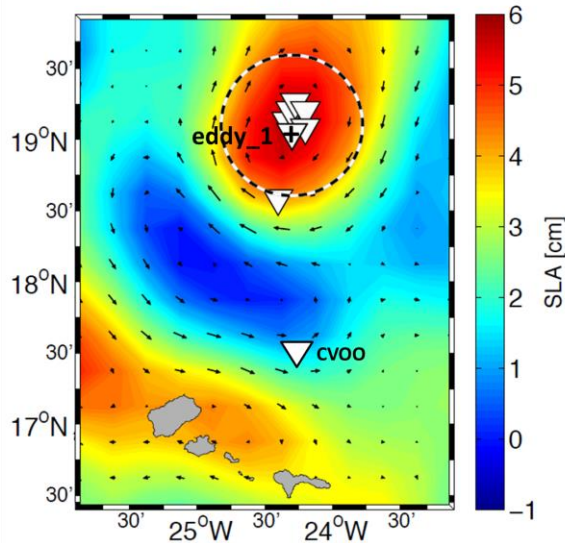
- 820 Wang, Q., Garrity, G. M., Tiedje, J. M., and Cole, J. R.: Naïve Bayesian Classifier for Rapid
821 Assignment of rRNA Sequences into the New Bacterial Taxonomy, *Appl. Environ. Microbiol.* ,
822 73, 5261-5267 doi: 10.1128/AEM.00062-07, 2007.
- 823 West, N. J., Lebaron, P., Strutton, P. G., and Suzuki, M. T.: A novel clade of *Prochlorococcus*
824 found in high nutrient low chlorophyll waters in the South and Equatorial Pacific Ocean, *ISME J*,
825 5, 933-944, 2011.
- 826 Wright, J. J., Konwar, K. M., and Hallam, S. J.: Microbial ecology of expanding oxygen minimum
827 zones, *Nat. Rev. Microbiol.*, 10, 381-394, 10.1038/nrmicro2778, 2012.
- 828 Yu, Y., Lee, C., Kim, J., and Hwang, S.: Group-specific primer and probe sets to detect
829 methanogenic communities using quantitative real-time polymerase chain reaction, 89, 670–679,
830 10.1002/bit.20347, 2005.
- 831 Zhu, M., and Ghodsi, A.: Automatic dimensionality selection from the scree plot via the use of
832 profile likelihood, *Computational Statistics & Data Analysis*, 51, 918-930,
833 10.1016/j.csda.2005.09.010, 2006.
- 834 Zuur, A. F., Ieno, E. N., Walker, N. J., Saveliev, A. A., and Smith, G. M.: Mixed effects models
835 and extensions in ecology with R, *Statistics for Biology and Health*, edited by: Gail, M.,
836 Krickeberg, K., Samet, J. M., Tsiatis, A., and Wong, W., Springer, 2009.
- 837
838

A



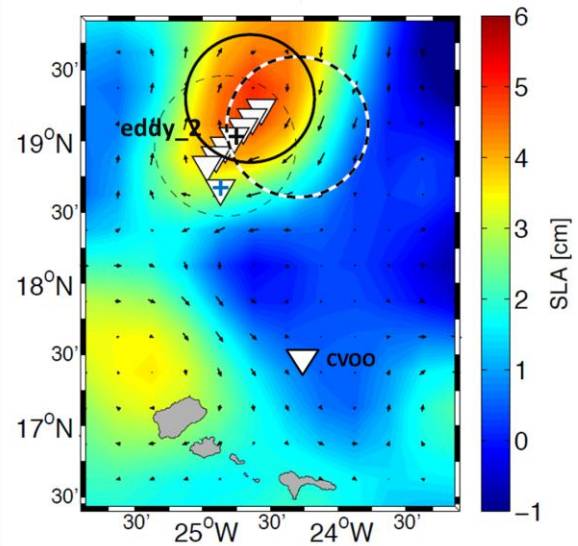
B

March 6, 2014



C

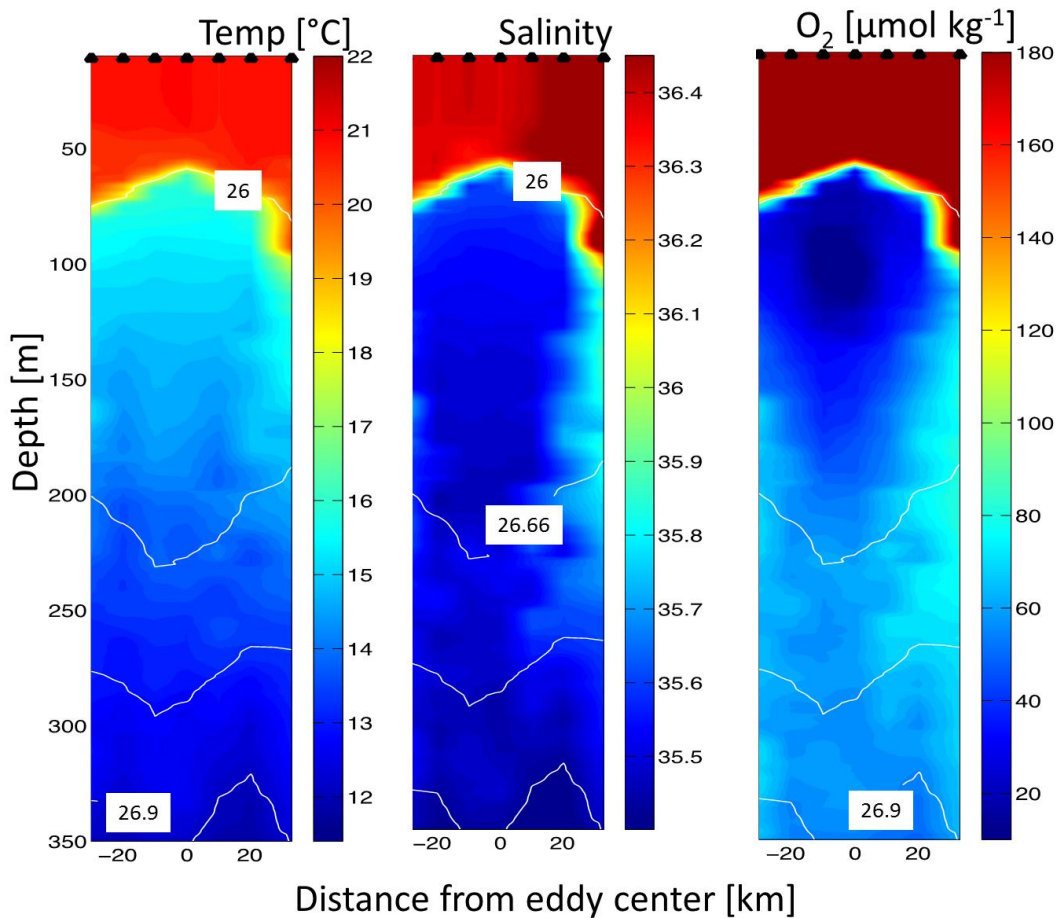
March 18, 2014



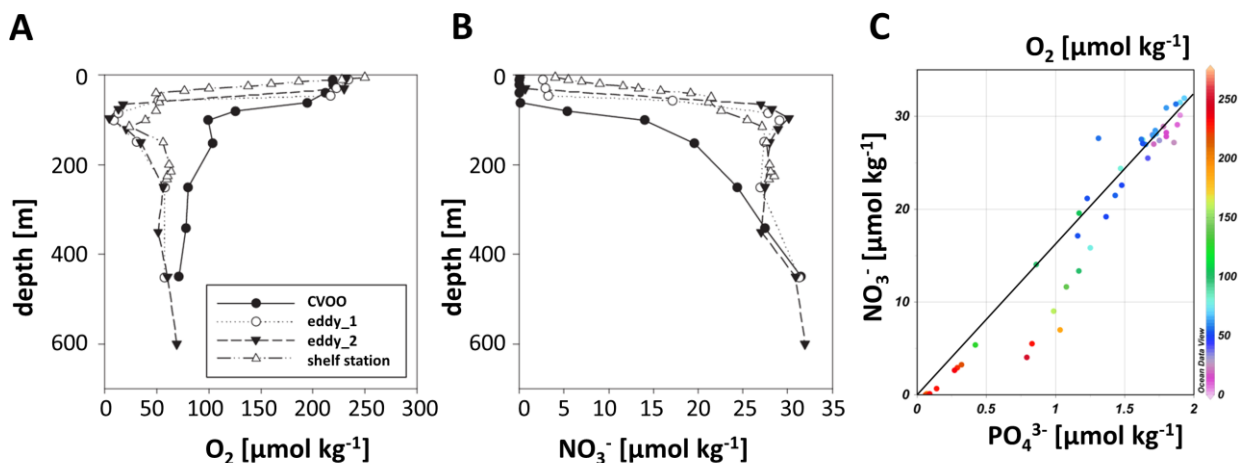
840

841 **Figure 1:** (A) MODIS-Aqua 4-km monthly mean chl *a* distribution in the ETNA (mg m⁻³) in November
 842 2013. Markedly increased chl *a* concentrations are associated with the low-oxygen ACME, located
 843 between 21°W and 22°W and 17.5°N and 19°N. Analyses and visualizations were produced with the
 844 Giovanni online data system, developed and maintained by the NASA GES DISC.

845 Eddy location indicated by sea level anomaly (SLA) during the time of the two surveys: (B) First eddy
 846 observation; + denotes the eddy_1 station, (C) Second eddy observation + denotes the eddy_2 station, an
 847 additional station was sampled at the eddy rim for C uptake measurements, indicated by the blue + White
 848 triangle marks the sampling station for the potential source water of the eddy. The dashed circles indicate
 849 the location of the eddy during the RV Islandia survey, the black circle indicates the eddy location during
 850 the RV Meteor survey, and the dashed black line indicates the direction of eddy propagation. Sampling
 851 stations are shown with white triangles.
 852



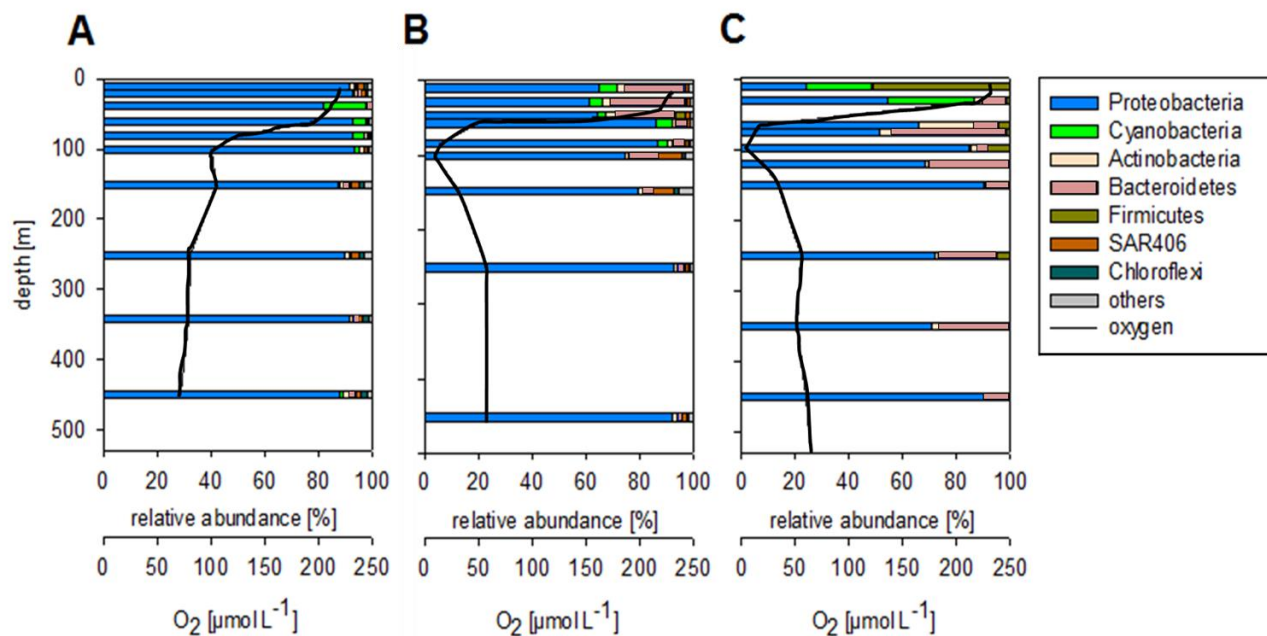
853
 854 **Figure 2:** Temperature (left panel), salinity (middle panel) and O_2 concentration (right panel) measured
 855 during a section of RV Meteor Cruise M105 across the studied eddy. Minimum O_2 was $4.8 \mu\text{mol kg}^{-1}$ at
 856 ~ 100 m water depth on that section; however, even lower O_2 was detected with a glider ($1.2 \mu\text{mol kg}^{-1}$).
 857 Isopycnals are indicated by white lines.
 858
 859



860
861

862 **Figure 3:** (A) O₂ and (B) nitrate (C) nitrite concentrations measured at the open ocean station CVOO
863 (black circles), in the first observation (eddy_1, open circles), second observation (eddy_2, black
864 triangles) and on the Mauritanian shelf (open triangles). (D) Nitrate vs. phosphate concentration at the 4
865 sampling stations. The color code denotes the O₂ concentration and the black line indicates the Redfield
866 ratio of N:P = 16:1.

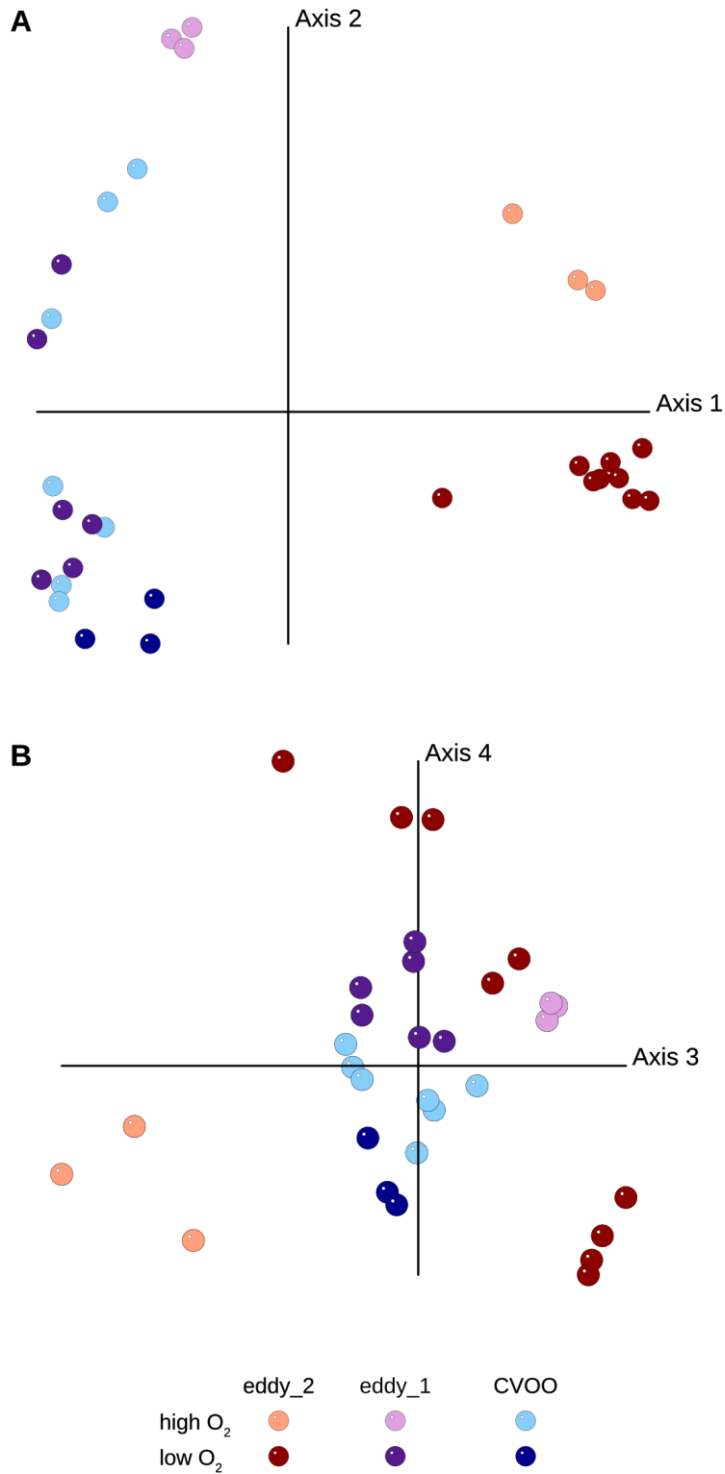
867



868

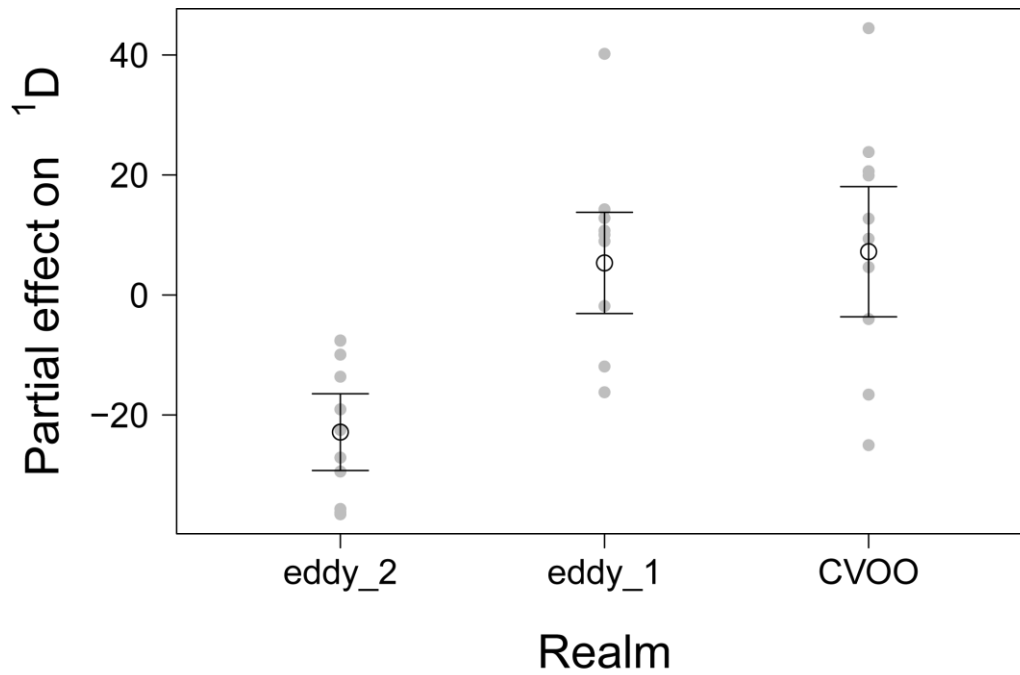
869 **Figure 4:** Distribution of bacterial phyla along vertical profiles of (A) CVOO, (B) first observation
870 (eddy_1) and (C) second observation (eddy_2) is shown along with the O₂ gradient (black line). Datasets

871 result from 16S rDNA amplicon sequencing (an overview on archaeal sequence distribution is given in the
872 supplemental material).

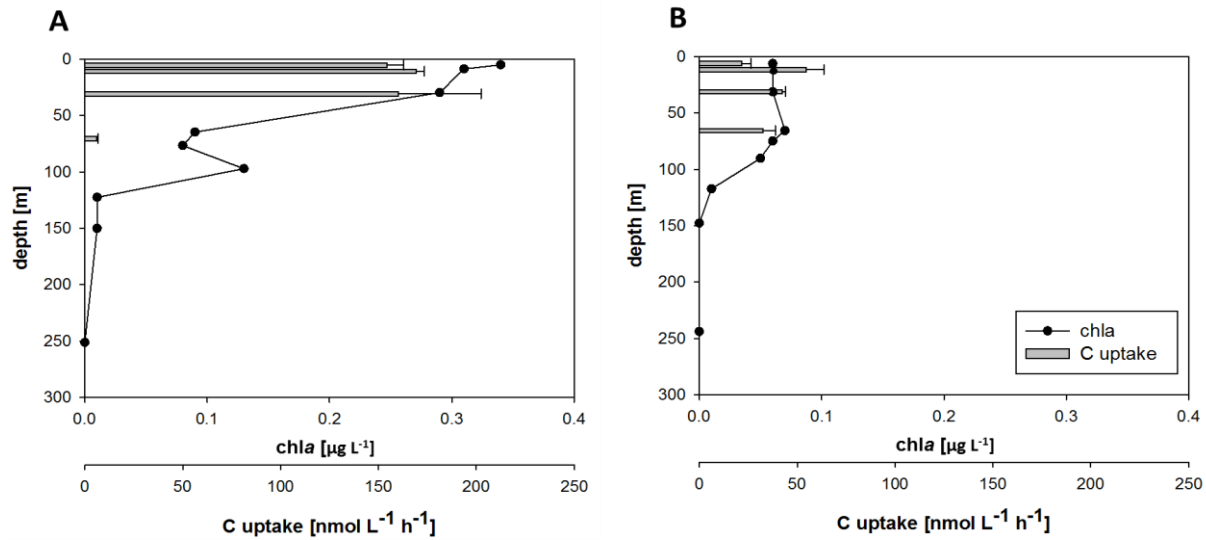


873
874 **Figure 5:** Redundancy analysis (RDA) of OTU distribution in samples from the first eddy observation
875 (eddy_1), from the second eddy observation (eddy_2) and from CVOO based on 16S rDNA sequences.
876 (A) First and second axis, (B) third and fourth axis of the RDA model, illustrating the interaction effect of

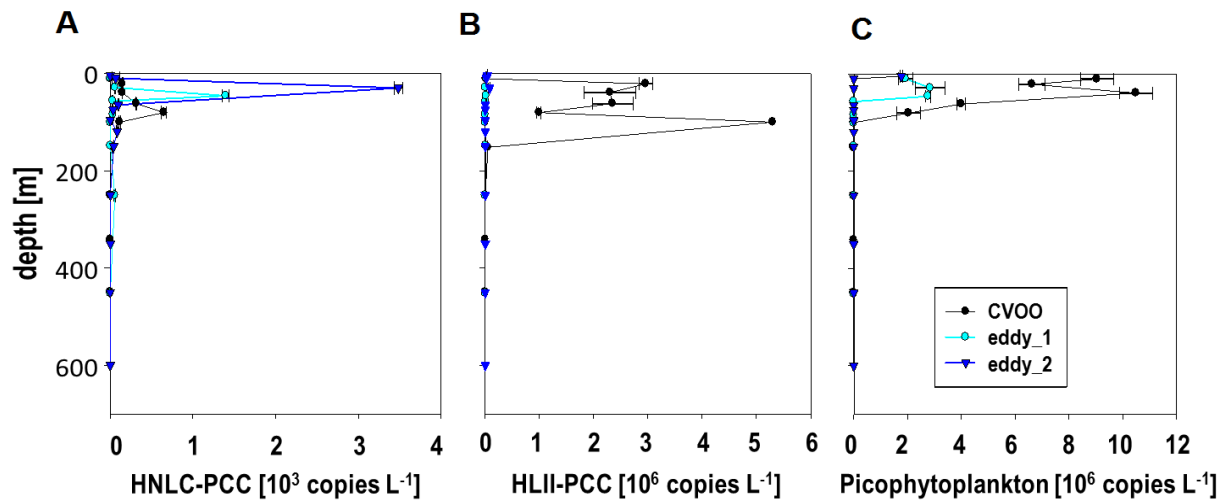
877 factor “Realm” and O₂ concentration. For plotting, the continuous variable “O₂” was converted into a
878 factor with two levels “high O₂” (>90 μM) and “low O₂” (≤90 μM).
879



880
881 **Figure 6:** Alpha diversity analysis of eddy sampling stations (first observation (eddy_1), second
882 observation (eddy_2)) and CVOO expressed as Shannon numbers equivalent (¹D). A strong and
883 significant decrease in diversity is observed in the eddy. Partial response residuals (black symbols) were
884 extracted from full GLS model re-fitted without the “Realm” main effect. Predicted values for partial
885 residuals modelled by the “Realm” main effect alone (and thus adjusted for differences in O₂
886 concentration) are shown as blue symbols. Error bars represent 95% confidence interval for fitted values.
887

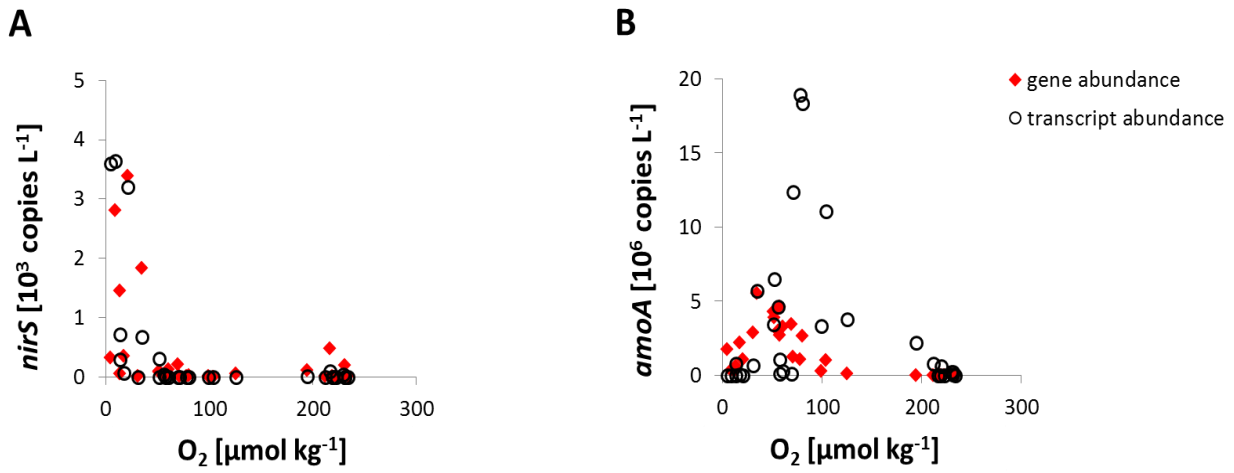


888
 889 **Figure 7:** Chlorophyll *a* (*chl a*, $\mu\text{g L}^{-1}$) distribution as determined from discrete measurements and carbon
 890 uptake rates (A) inside the eddy (eddy_2, second observation) and (B) at the eddy rim (location denoted in
 891 Fig. 1). Error bars indicate the standard deviation of three replicate samples for C uptake.
 892
 893



894
 895 **Figure 8:** Vertical distribution of *Prochlorococcus* and *Synechococcus* ecotypes quantified by qPCR.
 896 While the HNLC-PCC (A) dominates the eddy water mass and increases from the first observation
 897 (eddy_1) to the second observation (eddy_2) it is nearly absent outside the eddy (CVOO). HLII-PCC (B)
 898 occurs in highest abundances outside the eddy, while being close to the detection limit inside the eddy. (C)
 899 shows the distribution of pico-phytoplankton as detected with a general primer-probe system (Suzuki et
 900 al., 2001).

901



902

903 **Figure 9:** Gene and transcript abundance vs. O_2 concentrations of samples from the eddy observations
904 (eddy_1 and eddy_2) and CVOO. (A) shows the key gene for denitrification, *nirS*, coding for the nitrite
905 reductase, (B) shows archaeal *amoA* as key functional gene of ammonia oxidation, coding for the
906 ammonia monooxygenase. Gene abundances are denoted in red, transcript abundances are indicated by
907 black circles.